

MASTER OF SCIENCE THESIS

Drawing behavior of UHMWPE films made from solution casting: Influence of solvent quality

Sachin Kumar Enganati



Drawing behavior of UHMWPE films made from solution casting: influence of solvent quality

MASTER OF SCIENCE THESIS

For obtaining a degree of Master of Science in Aerospace Engineering at Delft University of Technology

Author: Sachin Kumar Enganati

Supervisors: Dr.ir. Peter Roozemon

Dr.ir. Roel Marissen

Dr.ir. Otto Bergsma

Dr. Roman Stepanyan

Dr.ir. Luna Imperiali

Date: 30/08/2016

Student Number: 4409426

Contact information: schn.ngnt@gmail.com

Summary

Ultra-High Molecular Weight Polyethylene (UHMwPE) fibers are well known for their very high specific mechanical properties such as tensile strength and Young's modulus. The solution spinning/solid state drawing process invented in the late 70s at DSM enables the production of these UHMwPE fibers with outstanding mechanical properties. Fibers with breaking strength greater than 3 GPa and modulus greater than 100 GPa are produced commercially nowadays. However, the strength of the aliphatic C-C backbone bond in polyethylene has been estimated to a value of 30GPa [45], whereas UHMwPE fibers strength in practice is only around 3GPa. And also these fibers are extensively used in bullet-proof vests which typically require an improved strength, preferably the ultimate. Hence, improving the mechanical properties of UHMwPE fibers is a key area of research in fiber technology.

The mechanical properties of UHMwPE fibers mainly tensile strength and modulus are directly proportional to the maximum achievable draw ratio (λ_{\max}) of the fibers [3]. This project was aimed to improve the maximum draw ratio of UHMwPE fibers which in turn enhances the mechanical properties. Recently it was published [33] that maximum draw ratio (λ_{\max}) can be improved by decreasing the solvent quality i.e. modifying the solvent in the production of UHMwPE fibers might be a way to achieve higher properties. Thus, the focus of this project is mainly to study the influence of different solvents on the production of high strength UHMwPE films/fibers. The solution/gel casting process was used to produce UHMwPE films as this process is well controllable, cheaper, and very much feasible in lab scale.

This project is divided into two parts. In the 1st part of study, few reference solvents will be considered to substantiate the literature results [33]. Next the following ways will be used to decrease the quality of the solvent to gel cast films and then the effect of this solvent quality on the drawing properties will be determined.

- Various blend compositions of a good solvent and a non-solvents.
- [REDACTED]

Subsequently, the investigation on the possible reasons for the increment in maximum draw ratio with decrease in solvent quality will be analyzed. [REDACTED]

[REDACTED]

Then in the 2nd part, preliminary study of some of the selected solvents on the production of UHMwPE fibers will be done. The drawing results will be analyzed to have an insight of translation from gel casting (films) to solution spinning (fibers) process. Based on the drawing results, chain kinetics and effect of quenching rate will also be examined.

Acknowledgement

This master's thesis represents the conclusion of my time as a student at Aerospace Engineering at TU Delft. I have presented my work with commitment and I hope you will have a good time reading it.

Firstly, I owe deep gratitude to Dr.ir. Harm van der Werff for introducing me to DSM. I am grateful to number of people at DSM, especially my supervisors Dr.ir. Peter Roozemon, Dr. Roman Stepanyan, Dr.ir. Roel Marissen, Dr. Luna Imperiali and Dr. Luigi Balzano. I thank you all for believing in my abilities and giving me the opportunity to carry out my thesis at DSM. Your guidance and constant motivation has helped me immensely and has been a continuous source of motivation throughout my thesis. I would like to thank my TU Delft supervisor Dr.ir. Otto Bergsma for his support and guidance during this thesis.

Furthermore, I would like to thank Rob Dassen and Har Graus for their endless assistance in explorative lab; Robbert van-Sluijs and Danny Driessen for DSC, Rheology experiments; Anouk Graven-van-Claassen for DMTA measurements; Jean Goossens for his assistance on drawing and tensile testes; Peter Boonen and Franks Brants for the spinning operations. A special acknowledgement also goes to my fellow interns at DSM: Jessica, Mike, Giulio, Jorgo, Max and Predrag with whom I have shared an incredible experience at DSM. I thank all of you for the help towards my thesis and making the working hours so much more interesting. I would also like to thank all my friends at ASM group, with whom I had a wonderful time during the first year of my MSc.

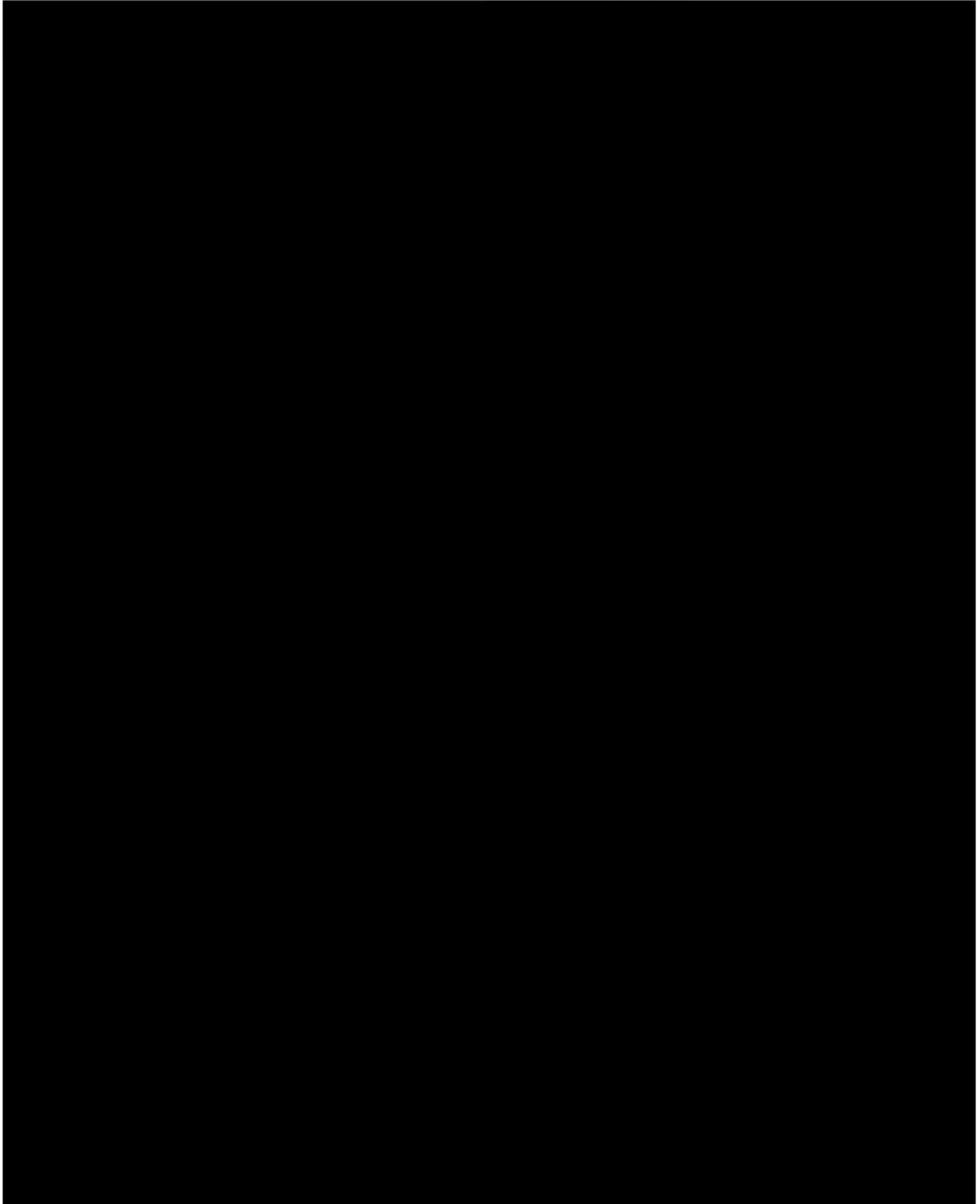
Lastly, I would like to thank my parents: my family Satyanarayana Rao and Rama Enaganti for giving birth to me at the first place, supporting me and being there for me all time.

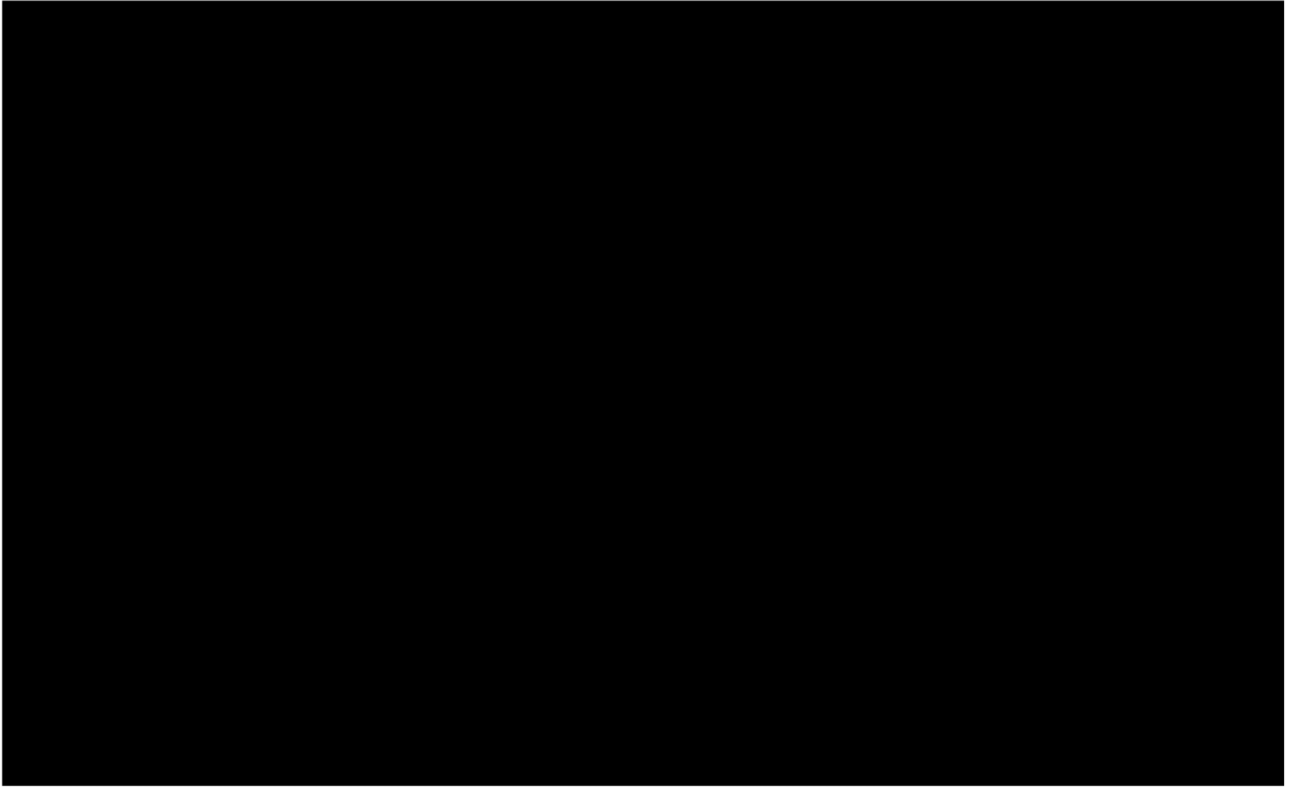
Table of Contents

Summary	4
Acknowledgement	5
List of Figures	8
List of Tables	10
Nomenclature	11
1. General Introduction.....	12
1.1. Introduction.....	12
1.2. Literature review	12
1.2.1. Overview of UHMWPE	13
1.2.2. Internal structure of UHMWPE fibers.....	15
1.2.3. Drawing characteristics of UHMWPE fibers.....	16
1.2.4. Effect of drawability on mechanical properties of UHMwPE fibers	17
1.2.5. Solvent concentration route to improve the drawability of UHMwPE fibers.....	18
1.2.6. Basics of solvent quality	20
1.2.7. Alternative solvent route to improve the drawability of UHMwPE fibers.....	22
1.3. Objective	23
2. Materials and Experimental procedures for UHMwPE films	25
2.1. Materials for the production of films.....	25
2.1.1. Experiment A - Effect of solvent quality on the drawability	25
2.1.2. Experiment B - blends of a good solvent and non-solvent to vary the solvent quality	26
2.1.3. Experiment C - variation of alkyl chain length to decrease the solvent quality ..	26
2.2. Methods.....	28
2.2.1. Differential scanning calorimetry.....	28
2.2.2. Gel casting process	30
2.2.3. Solvent removal process	32
2.2.4. Hand drawing process.....	34
2.2.5. Dynamic Mechanical Thermal Analysis	35
2.2.6. Rheological analysis.....	36
2.2.7. Morphological analysis - scanning electron microscope.....	38

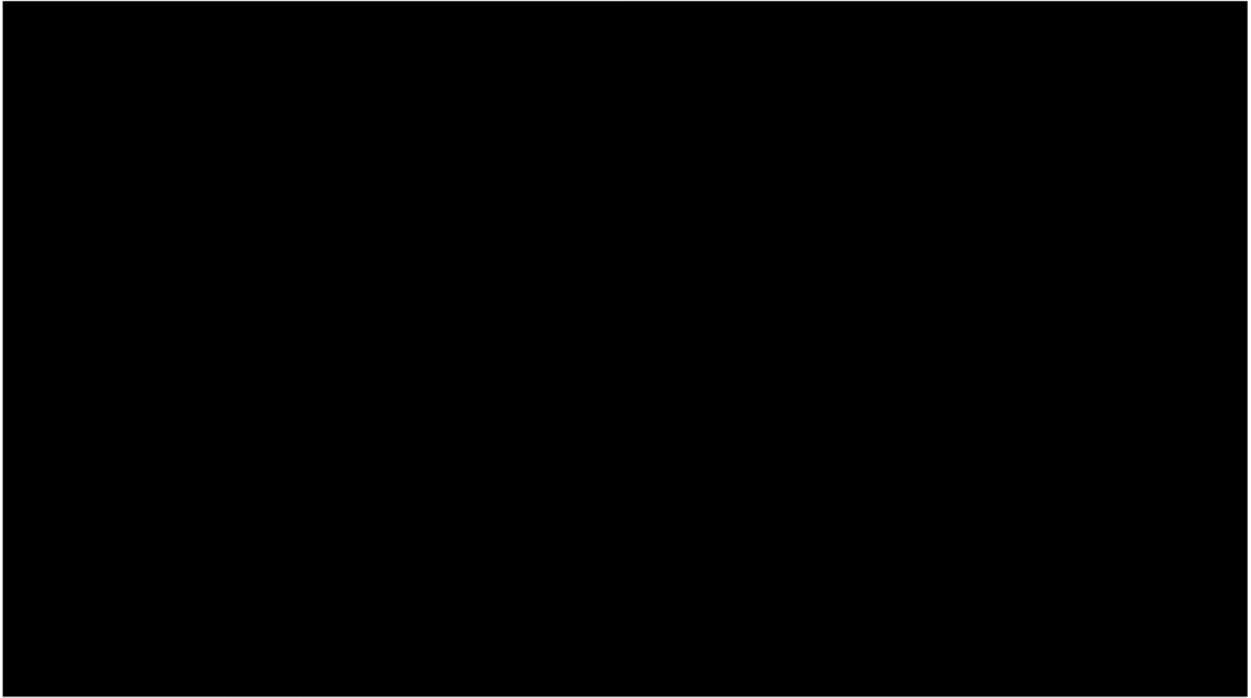
2.2.8. Morphological analysis - X-ray diffraction	40
3. Materials and Experimental procedures for the production of UHMwPE fibers.....	42
3.1. Materials	42
3.2. Methods.....	42
3.2.1. Solution spinning process.....	42
3.2.2. Solvent removal process	43
3.2.3. Solid state drawing	44
4. Results and discussion of UHMwPE films.....	45
4.1. Experiment A - effect of solvent quality on the drawability	45
4.2. Experiment B - blends of a good solvent and non-solvent to vary the solvent quality.....	46
4.3. Experiment C - variation of alkyl chain length to decrease the solvent quality	48
4.4. Mechanical properties	50
5. Results and discussion of UHMwPE fibers	51
5.1. Drawing results	51
5.2. Chain kinetics.....	52
6. Conclusions and Recommendations	54
7. References.....	56
Appendix A - Mechanical properties of DD1 fibers.....	59
Appendix B - SEM of DD1 fibers.....	62
Appendix C - Solvent extraction process in DD1 fibers.....	63
Appendix D - Dissolution (flask) experiment	64

List of Figures





List of Tables



Nomenclature

Acronyms

UHMWPE	Ultrahigh Molecular Weight Polyethylene
LMWPE	Low Molecular Weight Polyethylene
LMWPP	Low Molecular Weight Polypropylene
HDPE	High Density Polyethylene
LDPE	Low Density Polyethylene
PE	Polyethylene
amu	Atomic mass unit
M_w	Weight average molecular weight
M_e	Molecular weight between the entanglements
PO	paraffin oil
SA	Stearic acid
T_m	Melting point of the mixture
UDY	Un-Drawn Yarn
PDY	Partially Drawn Yarn
FDY	Fully Drawn Yarn
DD	Drawdown

List of Symbols

Symbol	Unit	Description
λ	-	Draw Ratio
λ_{max}	-	Maximum Draw Ratio
ϕ	%	PE Concentration
E	GPa	Storage Modulus
G^*	GPa	Complex Shear Modulus
δ	$^{\circ}\text{C}$	Phase angle
L_p	nm	Long period
L_c	nm	Crystal thickness

1. General Introduction

1.1. Introduction

Dyneema® is a super strong manmade fiber made from Ultra High Molecular Weight Polyethylene (UHMWPE) with a molecular weight between 2 – 6 million amu. The common Dyneema® grade SK75 has a Young's modulus of 125 GPa, strength of 3.6 GPa. It is 15 times stronger than steel but lighter than water, making it the strongest fiber on weight basis. The key to obtain outstanding mechanical properties is to align all chains (thus C-C bonds are loaded), so that the mechanical properties become highly unidirectional.

These fibers are made by so called solution spinning process [1, 2], i.e. first dissolving the UHMwPE powder in a solvent in order to reduce both the melt viscosity and entanglement density followed by cooling and solid state drawing at elevated temperatures. Hence, the maximum attainable draw ratio (λ_{\max}) can be achieved by the later step. Kanamoto et al. [3] have proved that the tensile strength and Young's modulus are directly proportional to the maximum draw ratio (λ_{\max}) achieved.

Therefore, it is essential to reach higher draw ratios to improve the tensile strength and modulus. It is well known that the λ_{\max} is governed by entanglement density [46] and can be increased by decreasing the polymer fraction in the gel mixture [4]. Thus superior mechanical properties can be obtained at very low polymer concentrations. However, this has disadvantages such as the difficulties in recovering and purifying excess of the remaining solvent (on a commercial scale, the quantity of solvent needed for producing 100kg of fibers is around 900kg which is already a colossal amount to recover). These solvents are also flammable which may lead to environmental and health hazards.

According to Tervoort et al. [33] an alternative way of increasing λ_{\max} in the production of UHMwPE fibers is by modifying the solvent in the gel (traditional solvents are decahydronaphthalene (decalin) and paraffin oil). The selected solvent must be relatively poor as compared to decalin or paraffin oil. The main goal of this project is to understand this poor solvent effect on the drawability of the UHMwPE films/fibers. To accomplish this objective firstly the solvent quality is varied systematically and its effect on the drawability of UHMwPE films was studied.

was also carried out on different solutions to understand the role of entanglement density. Finally, spinning experiments were performed to produce UHMwPE fibers in various solvents and drawing results were analyzed.

1.2. Literature review

The general aim of this thesis will be to investigate the effect of different solvents on the production of high strength UHMWPE films/fibers and also to understand the drawing behavior in the selected solvents. For this purpose a short literature review will be provided in this section on some relevant concepts. Firstly a general overview, description on the internal structure and drawing behavior of UHMWPE fibers will be

provided, as the study of the deformation behavior of UHMWPE would require an understanding of its internal structure. Then, we shall look into some important factors influencing the drawing behavior of UHMWPE fibers and then towards understanding the effect of solvent quality on drawing behavior. Finally, a brief description will be provided on improving the drawing properties by using other alternative solvents from literature, furthermore the proposed objective to carry out the project will be discussed.

1.2.1. Overview of UHMWPE

Polymers are long molecules consisting of many small monomers [5]. The main characteristic feature of polymers is that they consist of many of these extremely large molecular chains, with molar masses of 10^4 g/mol or even more. Because of these long chains a lot of entanglements (contact between chains) are present in the material and are important for the behavior of the polymer as a whole certain. Polymers can crystallize but are never fully crystalline like metals. They typically consists of both amorphous and crystalline domains in which case they are called semi-crystalline. The properties of polymers and polymeric fibers depend strongly on the degree of molecular orientation and the level of crystallinity. Polymers with microcrystalline regions are generally tougher and have more impact-resistant than totally amorphous polymers [6]. Polymeric fibers typically possess high strengths and moduli of elasticity. This in combination with low weight makes polymeric fibers very useful for many applications.

Ethylene (C_2H_4) is a gaseous hydrocarbon commonly produced by the cracking of ethane, which in turn is a major constituent of natural gas or can be distilled from petroleum [7]. Ethylene molecules are essentially composed of two methylene units (CH_2) linked together by a double bond between the carbon atoms - a structure represented by the formula $CH_2=CH_2$. Under the influence of polymerization catalysts, the double bond can be broken and the resultant extra single bond used to link to a carbon atom in another ethylene molecule. Thus, made into the repeating unit of a large, polymeric (multiple-unit) molecule known as polyethylene. The polyethylene molecule has a high degree of flexibility, thus the C-C bond in it can take many different configurations. It can be visualized as a polymer chain with a very long piece of string as shown in Figure 1.

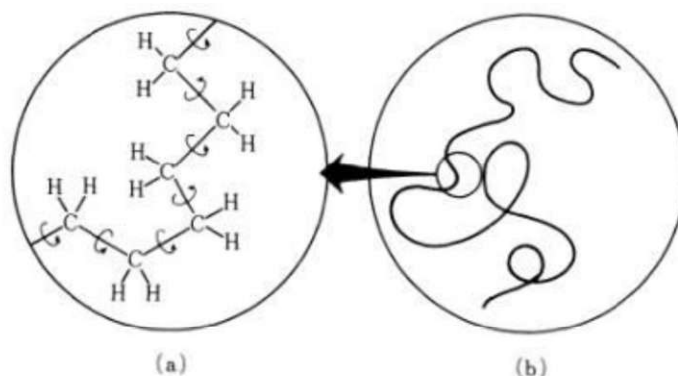


Figure 1: (a) Atomic structure of the polyethylene molecule. (b) An overall view of the molecule.[8]

Polyethylene grades are generally classified into three categories: low density polyethylene (LDPE) with long branches, linear low density polyethylene (LLDPE) with short branches and high density polyethylene (HDPE) composed of linear chains as shown in Figure 2. UHMwPE is a particular case of HDPE characterized by very long chains, with molar mass of above 10^6 g/mol, see Figure 3. The superior properties of the UHMwPE fibers are mainly due to a very high degree of orientation of those extremely long molecules.

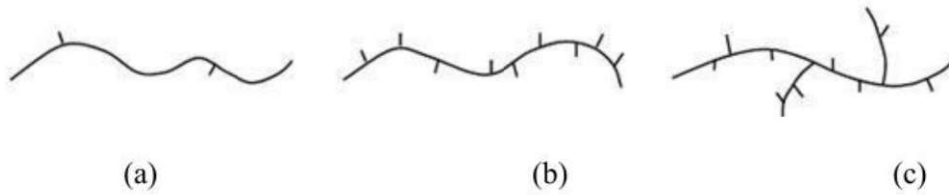


Figure 2: Schematic representation of (a) HDPE (b) LLDPE and (c) LDPE structures.

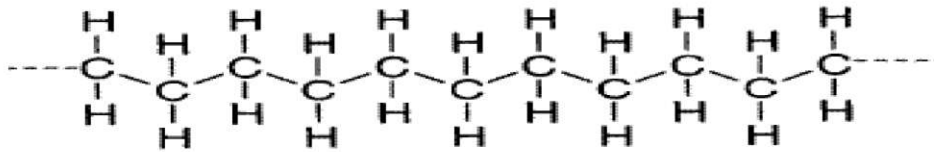


Figure 3: Molecular structure of UHMwPE [9]

The molecular weight of ethylene is 28.05 g/mol. The molecules within Dyneema® consist of about 10,000 to 100,000 of these monomers. Orienting these molecules in a way such that they lie nearly parallel to each other will result in a modulus that does not depend on the Van der Waals interactions but instead depends on the intermolecular, covalent forces which are much stronger than the Van der Waals forces. These Van der Waals forces between the molecules are more important for transferring the load between the polyethylene chains. The total force transmitted by these Van der Waals forces depends on the length of UHMwPE chains. To obtain the ultimate strength of the material, it is therefore important that UHMwPE molecules consist of very long oriented chains. The macromolecular orientation of high performance polyethylene (HPPE) and regular polyethylene is shown in Figure 4.

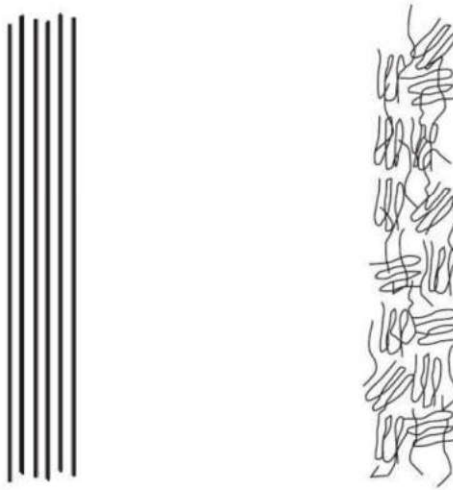


Figure 4 : Highly oriented polyethylene and a regular polyethylene (no orientation) [10]

1.2.2. Internal structure of UHMWPE fibers

A typical Dyneema® yarn consists of number of filaments. These filaments in-turn are comprised of macrofibrils or shishes which are semi-crystalline entities with long extended-chain crystals alternating in the fiber direction with less ordered domains [11]. From literature [12], only two models are able to determine the structure of macrofibrils. In the Continuous crystalline model, it is assumed that the shishes consist of almost continuous crystalline phase with scattered and limited defects. On the other hand, in macrofibrillar model, a shish is assumed to consist of highly extended chains forming crystalline microfibrils with a diameter ~15nm. The crystalline structure of Dyneema® filament can be visualized in Figure 5. The shishes are laterally connected by tie molecules running through the amorphous domains. Tie molecules can run transversally from one crystallite to another, this way also being a part of the disordered region and also longitudinally connecting crystallites.



Figure 5: Crystalline structure of Dyneema®

1.2.3. Drawing characteristics of UHMWPE fibers

Different routes have been explored to obtain these highly oriented structures such as melt-spinning [13, 14], solution-spinning using the Couette apparatus [15,16], and the surface-growth technique [17]. While the use of melt-spinning is limited by the molecular weight of the polymer, as the viscosity in the extruder is directly proportional to the molecular weight raised to the power 3.4. The other techniques are mostly limited by the quality and production speed of the filament. Only the process of solution-spinning using semi-dilute polymer solutions enables the commercial manufacturing of UHMwPE fibers. The dissolution of UHMwPE powder not only lowers the viscosity during extrusion but also reduces the amount of entanglements increasing the drawability afterwards [18].

After the production of UHMwPE filaments from gel/ solution spinning process, these filaments are stretched in ovens which is called as solid state drawing. The temperature at which this process takes place depends upon the melt temperature of UHMwPE fibers, because near this temperature the molecules are more mobile and therefore easier to orient. If the temperature is above the melt temperature, the filaments can be partially molten and loose the orientation due to relaxation. As the melting point of non –oriented UHMwPE is around 142⁰ C, in the first drawing step the temperature has to be below this value. Nevertheless, in the second drawing step the restriction is shifted to a higher value, as the melting point (increases) depending upon the orientation. From Equation 1, melting point is inversely proportional to entropy. The entropy decreases when the molecules start orienting ($\Delta S_2 < \Delta S_1$) resulting in higher melting temperature ($T_{m2} > T_{m1}$).

$$T_m = \frac{\Delta H}{\Delta S} \quad [1]$$

Here T_m is the melting temperature, ΔH is the change in Enthalpy and ΔS is the change in Entropy.

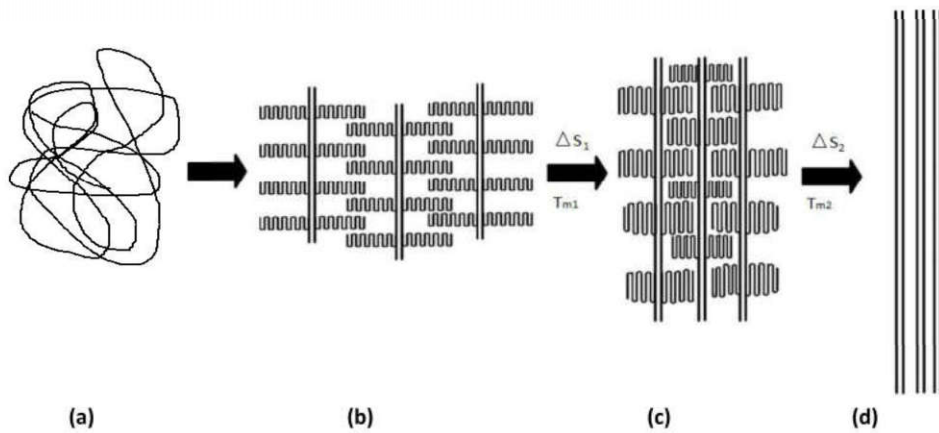


Figure 6: Schematic overview from amorphous to highly oriented UHMwPE [19].

The superior properties of the UHMwPE fibers are mainly due to a very high degree of orientation of those extremely long molecules. In a molten or a dissolved state, the polymer molecules possess no orientation and have a shape of a random coil, see Figure 6(a) [19]. When crystallized under flow conditions, they would typically end up in an oriented semi-crystalline state with chain-folded crystalline lamellae (kebab) attached to long extended chain crystals (shish), with characteristic structures shown in Figure 6(b), also called as shish-kebabs. Some amorphous material (not shown in the figure) is in between the lamellae. Upon further processing – drawing, the molecules are further oriented, as shown in Figure 6(c,d). Solid state drawing leads to an increased amounts of extended chain crystals while the amount of the amorphous phase, or non-oriented material, is dramatically reduced. It was also found that during the solid start drawing, the kebabs transform into shishes and the distance between shish-kebabs decreases [20]. Not all kebabs can be fully transformed into a shish and connect the shishes (tie molecules). The current view of the final morphology is based on a two-phase model. In this model a filament consists of a number of micro fibrils and these micro fibrils are located in a pseudo-amorphous matrix.

To summarize, orientation of molecules is very important to make high performance UHMwPE fibers. A highly oriented crystalline material is much stronger than non-oriented material. This is due to the fact that in an oriented PE the mechanical load is carried by strong covalent bonds, whereas in non-oriented PE the mechanical load is mainly carried by much weaker Van der Waals forces. Thus the high strength and modulus of UHMwPE fibers originate from the fact that the macromolecules are oriented in the fiber direction, so that the great strength of the covalent bonding along the chain axis is utilized [22]. In PE, the strength of the aliphatic C-C backbone bond has been estimated to a value of 30GPa, whereas UHMwPE fibers strength in large scale commercial practice is only around 3 GPa. This indicates the ample scope to improve the fiber properties stimulating the objective of this project.

1.2.4. Effect of drawability on mechanical properties of UHMwPE fibers

The maximum draw ratio (λ_{max}) can be governed by solid state drawing after the production of these fibers. The maximum attainable draw ratio will define the maximum tensile strength and Young's modulus of the UHMwPE fibers as shown in Figure 7. Kanamoto et al. [23] have studied the relation between tensile strength and Young's modulus with draw ratios, for different polyethylene grades. It was found that draw ratio of the fiber is directly proportional to the tensile strength and modulus and reaches a plateau after certain maximum draw ratio. It was also found that maximum tensile strength is limited by the molecular weight of PE (see Figure 7b). Hence it is desirable to use very high molecular weight polyethylene for producing high strength fibers. It is also advantageous to get higher draw ratios without lowering concentration not only for making high strength fibers but also for other specialty grades like low creep grades (which are also harder to draw when compared to standard fiber grades of polyethylene used).

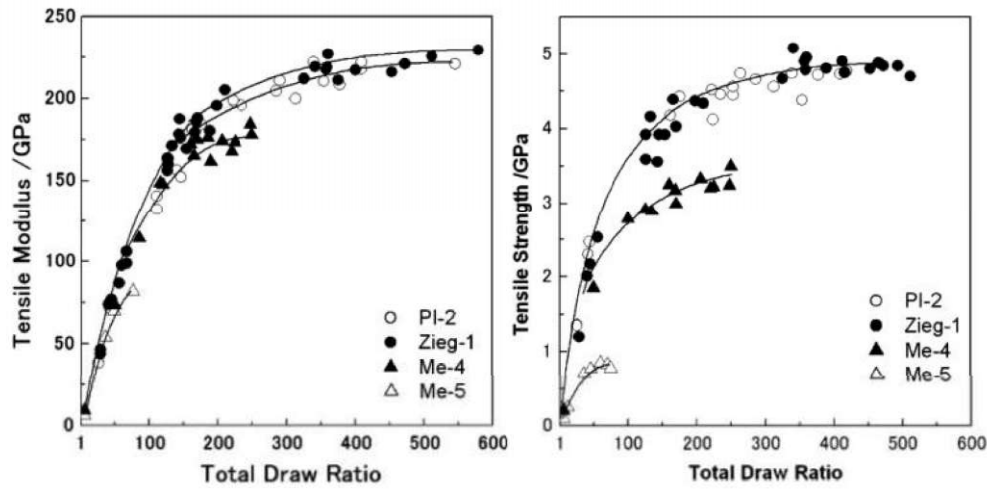


Figure 7: (a) Modulus and (b) Tensile strength as function of Total Draw ratio [23]

1.2.5. Solvent concentration route to improve the drawability of UHMwPE fibers

Smith et al. [24, 25] studied the influence of the solvent concentration on the drawability of UHMwPE filaments processed by solution spinning in dilute and concentrated solutions. It was observed that the maximum attainable draw ratio achieved in solution spinning process is very high when compared to fibers made from melt spinning [10]. It was seen that when filaments were made with concentrated solutions consisting of 10-50 wt% of solvent, the maximum attainable draw ratio was similar to that in the case of melt spun fibers at the same temperature, which is drastically lower than the draw ratios obtained from dilute solutions (see Figure 9). Hence, it clearly indicates that decreasing the solvent concentration has a negative effect on the achievable maximum draw ratio of the UHMwPE fibers processed from solution spinning/drawing [5].

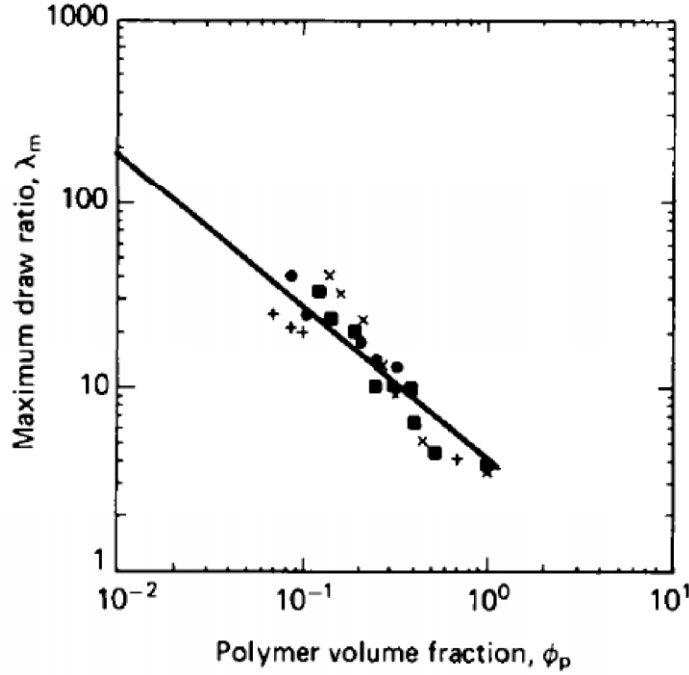


Figure 9: Comparison of maximum draw ratios versus initial polymer volume fraction [48]

Thus the maximum attainable draw ratio is inversely proportional to the square root of initial polymer concentration in solution (Figure 9). This can be physically interpreted by considering entanglement as permanent crosslinks which limits draw ratio. It is assumed that entanglements are trapped in polyethylene upon crystallization and act as semi-permanent crosslinks in a physical network upon solid state drawing. Experimental analysis has given a relation between the maximum draw ratio (λ_{max}) of UHMwPE which is crystallized from the solution containing different amounts of polymer and on the initial volume fraction of polymer as shown in Equation 2. The deformation behavior of UHMwPE at elevated temperatures is dominated by the number of entanglements [26]. Nevertheless, the entanglement density is independent of the solvent quality for good solvents in concentrated regime.

$$\lambda_{max} = \lambda_{max^1} \times \left(\frac{1}{\phi}\right)^{0.5} \quad [2]$$

Here λ_{max^1} is the maximum draw ratio of melt quenched/crystallized material and ϕ is the concentration of the polymer in the solution. From Equation 2, it is very clear that to improve drawability or maximum draw ratio of UHMwPE fibers, the polymer volume concentration in the solution needs to be decreased. Although this is possible to a certain degree (economically feasible) but it was preferred to spin at higher concentrations (economically more feasible). Therefore, the industries producing UHMwPE fibers in economical scale have chosen polymer concentration around 10% v/v, which leads to relatively lower mechanical properties due to its higher polymer concentration in the solution spinning process.

1.2.6. Basics of solvent quality

In order to understand the effect of alternative solvents on the drawability of high strength UHMwPE fibers, first let us look into the basics of polymer-solvent systems. Firstly, depending upon the concentration of the polymer used, three different cases are possible in any polymer-solvent system as shown in Figure 8. Here, c^* is the critical overlap concentration of polymer coils and is one of the most important characteristic values of a polymer solution. Graessley [27] provided a simple definition of c^* that is widely accepted for demarking the boundary separating the physical and rheological definition of dilute and semi dilute polymer solutions [44]. This can be seen in Equation 3:

$$c^* = \frac{0.77}{[\eta]} \quad [3]$$

where $[\eta]$ is the intrinsic viscosity of the polymer solution which depends on the molar mass of the chain according to the Mark-Houwink-Sakurada equation $[\eta] = K_{[\eta]} M^a$, where $K_{[\eta]}$ is a constant and the power-law index $0.5 \leq a \leq 0.8$ varies with the quality of the solvent. Thus, the value of C^* of a system predominantly depends on the solvent employed. To have an idea of C^* value, for polymer solution polyethylene and decalin is around 0.1 wt%.

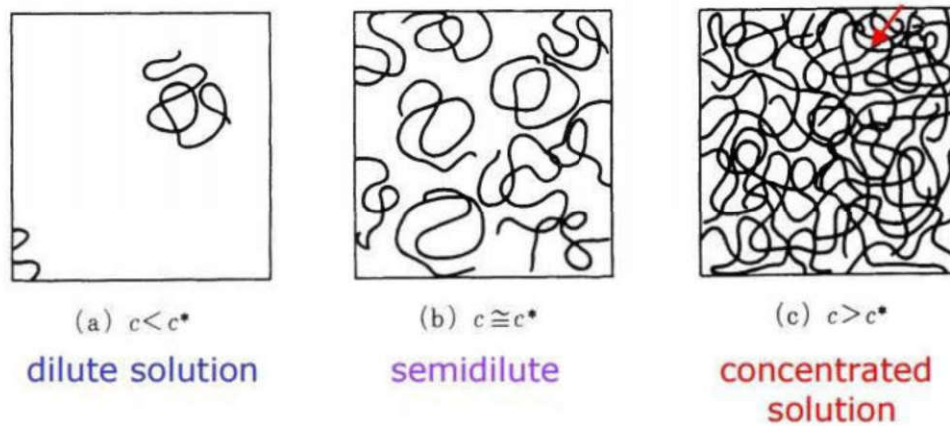


Figure 8: Concentration regimes of polymer solutions

Now, let us understand the dilute solution systems of a specific polymer in different solvents. The solubility of polymer in solvent not only depends on the kind of solvent employed, but also on the temperature, and the molecular weight of the polymer. The polymer-solvent interactions play an important role in this case, and its magnitude, from a thermodynamic point of view, will be given by the solvent quality. Simply, the quality of the solvent depends on the energy of mixing, which is

$$\Delta G_m = \Delta H_m - T^* \Delta S_m \quad [4]$$

Thermodynamically, for a solvent to be good, the free energy of mixing should be negative. According to Flory-Huggins theory [28], the above equation 4 can be expressed as

$$\frac{\Delta G_m}{n} = kT \left(\frac{\Phi}{N_A} * \ln \Phi + \frac{1-\Phi}{N_B} * \ln(1 - \Phi) + \underbrace{X * \Phi * (1 - \Phi)}_{\text{Enthalpy term}} \right) \quad [5]$$

Entropic term
Enthalpy term

Here k is Boltzmann constant, T is temperature, Φ is polymer concentration, n is total number of lattice sites in the model, N_A is the number of lattice sites for polymer and finally X is the Flory-Huggins interaction parameter (chi parameter). Here the entropic term contribution always promotes mixing but the enthalpy term may promote or hinder mixing depending upon the chi parameter. Thus, from Equation 5, it can be understood that the sign of ΔG_m is predominantly dependent on the sign of chi parameter (X) which are directly proportional to each other. For a solvent to be good, ΔG_m should be negative implying X to be negative. Hence, it should be inferred that the solvent quality is inversely proportional to X .

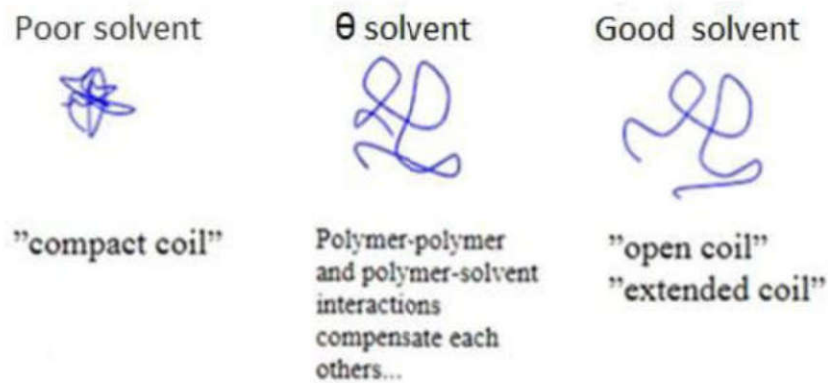


Figure 9: Schematic representation of different in solvent quality

Thus, in a "good" solvent, the solubility parameter is similar to that of the polymer, the attraction forces between chain segments are smaller than the polymer-solvent interactions; the random coil adopts an unfolded conformation. In a "poor" solvent, the polymer-solvent interactions are not favored, and therefore attraction forces between chains predominate, resulting in the random coil adopts a tight and contracted conformation [29].

In extremely "poor" solvents, polymer-solvent interactions are eliminated thoroughly, and the random coil remains so contracted that they eventually precipitates causing liquid-liquid phase separation. We say in this case, that the macromolecule is in the presence of a "non-solvent".

The particular behavior that a polymer displays in different solvents, allows the employ of a useful purification method, known as fractional precipitation. For a better understanding about how this process takes place, let's imagine a polymer dissolved in a "good" solvent. If a non-solvent is added to this solution,

the attractive forces between polymer segments will become higher than the polymer-solvent interactions. At some point, before precipitation an equilibrium will be reached, in which $\Delta G = 0$, and therefore $\Delta H = T\Delta S$, where ΔS reaches its minimum value. This point, where polymer-solvent and polymer-polymer interactions are of the same magnitude, is known as θ state and depends on: the temperature, the polymer-solvent system (where ΔH is mainly affected) and the molecular weight of the polymer (where ΔS is mainly affected).

It may be inferred then that lowering the temperature or the solvent quality, the separation of the polymer in decreasing molecular weight fractions is obtained. Any polymer can reach its θ state, either choosing the appropriate solvent (named θ solvent) at constant temperature or adjusting the temperature (named θ temperature or Flory temperature) in a given solvent.

On the other hand, in concentrated solutions, the number of contacts (entanglements) between the polymer chains does not depend on the solvent quality [30]. The regime we are interested is semi-dilute solutions, here when a poor solvent is used the extension of the polyethylene molecules in the solution decreases as compared with the case of using a good solvent. Consequently, it is considered that number of entanglements between the polymer chains decreases as the solvent quality decreases [33, 46] Then, according to the classical rubber theory, the maximum draw ratio of a cross linked network depends on the statistical chain units between the cross links (N_c) [26] as shown in equation:

$$\lambda_{max} \propto \sqrt{N_c} \quad [6]$$

This can be well correlated with:

$$\lambda_{max} \propto \sqrt{M_e} \quad [7]$$

Where M_e is the molecular weight between the entanglements.

Thus, in combination with above mentioned assumption and rubber theory, decrease in solvent quality can lead to the improvement in maximum draw ratio. However to prove this, M_e should be relatively high for poor solvents when compared with good solvents. The attempt to measure M_e in different solvents was made by shear rheology experiments in later stage of this work (see section 4.5). However, this hypothesis is the central point in order to choose the objectives of this project. Based on this assumption, couple of researches have been done which will be discussed in the next section.

1.2.7. Alternative solvent route to improve the drawability of UHMwPE fibers

The conventional extrusion process (melt spinning) halted for the production of Ultra High Molecular Weight Polyethylene fibers due to its high melt viscosity. Thereafter, *solution spinning* was introduced so that viscosity can be reduced by dissolving the UHMwPE in the solvent and also to have a control over the process. Even though the solution spinning process is very much successful in producing UHMwPE fibers with better properties, after the production of spun fibers, the petro chemical solvent must be removed

(evaporated) from the fiber which can be hazardous to health and environment. Smith et al. [33], Rajput et al. [31] proposed environment friendly process by using natural oils as solvent and eliminating the solvent extraction step. This is done by replacing the petrochemicals with environment friendly solvents, natural oils such as sunflower oil, palm oil and orange oil (terpene) for dissolving UHMwPE polymer [31]. Orange oil (terpene) was used for further gel spinning process. UHMwPE filaments were produced and terpene was removed by allowing the fibers to remain at room temperature for two days. This process made it more sustainable (terpene is obtained from renewable resources), reduced the costs involved in extraction of non-volatile solvents and reduced health and environmental hazards. Nonetheless, the fiber properties were not reported, which is the major concern on an economical scale.

Motooka et al. [32] successfully spun UHMwPE fibers at higher concentrations in different aliphatic compounds such as amides, esters, ketones, alcohols, acids etc. Unfortunately lower mechanical properties were achieved. Further, the extraction meant (washing agents for respective solvents) may result in environmental effects. In addressing these issues (using environmental friendly solvents and achieving ultra-high mechanical properties, Tervoort et al. [33] studied the gel spinning process of UHMwPE in different solvents which are poorer than decalin or paraffin oil. Note that all the solvents chosen were better than theta solvent but they are not as good as decalin. Here, rather than opting concentration route (varying UHMwPE % v/v) to control the entanglement density in the solution process, solvent 'quality' route was chosen. Surprisingly, it was found a drastic increase in the draw ratios with the new solvents (especially for stearic acid) compared to decalin case at a specific polymer concentration (typically around 10%v/v). However, the exact mechanism behind these astonishing results is yet unanswered which leaves an ample space for research. One possible mechanism is that during process of gelation of a solution at elevated temperature, the maximum draw ratios can be improved likely due to (additional) disentanglements due to "reeling in" of the polymer chains during the formation of crystalline entities [12, 26, 33]. The other could be entanglement density in a poorer solvent is lower, which would result in a higher draw ratio. Therefore, identifying an eco-friendly solvent for gel spinning of UHMwPE fibers (with improved mechanical properties) will be a breakthrough in fiber technology.

1.3. Objective

DSM Dyneema® is interested in optimizing the tensile properties even more, to further improve the performance of Dyneema® products by using more environmental friendly solvents. The aim of this research project will be investigating on the effect of solvent quality on the production of high strength UHMwPE films/fibers. The research will be mainly carried out on gel casting UHMwPE films with different solvents as it is well controllable, easy to act and to understand the behavior in lab scale. This objective can be achieved by the following sub goals.

1) How does the solvent quality effects drawing properties of UHMwPE films?

- Considering decalin as reference, number of solvents will be chosen by varying the quality of it.

- Simultaneously, melting point depression (T_m) of the solutions made with different selected solvents in UHMwPE will be determined. Here, the solvent quality can be checked experimentally, as the melting point of depression should be inversely proportional to the solvent quality.
- Gel casting process will be used to produce the UHMwPE films with various solvents. Thereafter drawing tests and evaluation of mechanical properties on the films will be done.

2) Does the solvent quality correlate to the achievable maximum draw ratio?

- The difference in entanglement density in the films of various solvents will be examined by rheological experiments. This is to understand the role the entanglements on drawability.
- Morphological analysis (SEM) will be done on the surface and cross section of this undrawn cast films to understand the morphology and crystallite structure differences with various solvents. XRD analysis was also performed to understand the crystal structure (crystallinity and crystal thickness) of the different UHMwPE films produced.

3) If these solvents can produce higher draw ratios as expected, then this process will be taken to the next level, by production of fibers with some of these selected solvents and estimating the mechanical properties.

2. Materials and Experimental procedures for UHMwPE films

2.1. Materials for the production of films

For the production of films, the basic polymer used was ultra-high molecular weight polyethylene. Its grade and properties were tabulated below. To find the best 'worst' solvent for improving the UHMwPE films/fibers properties, different hypothesis were considered as shown further in this section.

Polymer	Number average molecular weight Mn [g/mol]	Weight average molecular weight Mw [g/mol]	Polydispersity Index (PDI)	Melting point (T _m) [°C]
UHMwPE	-	-	-	142

Table 1: Properties of UHMWPE polymer

Here dbpc (2,6-Di-*tert*-butyl-*p*-cresol) was used as antioxidant (stabilizer), in order to avoid, as much as possible, the influence of degradation on drawing properties and thus to investigate only the influence of different solvents on it. Always 0.2% (w/w% based on solvent) will be added to the solution.

2.1.1. Experiment A - Effect of solvent quality on the drawability

Firstly, in order to analysis the effect of solvent quality on the mechanical properties of the UHMwPE films, solvents of less quality from the literature [31-34] were chosen as shown in Table 2.

Solvents	Commercial name	Quality
Decalin	-	Good solvent
Paraffin oil (PO)	-	Quite good
Stearic acid (SA)	-	Relatively poor solvent

Table 2: Reference solvents selected from literature

Here, good solvent indicates that polymer-solvent interactions are greater than polymer-polymer interactions in a solution. As the solvent quality decreases, the polymer-polymer interactions starts to raise and at certain point, both of these interactions becomes equal. It is called theta solvent. Stearic acid is quite close to this theta solvent. The objective was estimate the maximum attainable draw ratios of UHMwPE films in different solvents (different quality) at a specific concentration.

2.1.2. Experiment B - blends of a good solvent and non-solvent to vary the solvent quality

Successively, to explore new possibilities for alternative solvents, blends of a solvent and a non-solvent were made in order to reduce the solvent quality. Here, the hypothesis was *gradual* addition of a non-solvent to good solvent will decrease the quality of the solvent (implies improvement in maximum attainable draw ratio) to an extent, after certain composition the non-solvent behavior dominates resulting in liquid-liquid phase separation, see Figure 10.

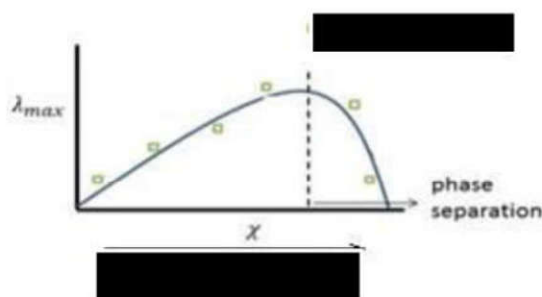


Figure 10: Maximum draw ratio as a function of solvent quality: experiment B

In Figure 10, x-axis indicates the chi parameter which is the measure of solvent quality (higher the chi parameter, lower the solvent quality). Note that the given figure and points in it are the replication of the assumption but not proven or not from literature. For experimental analysis, blends of decalin (as good solvent) and solvent A^[13] (as non-solvent) was chosen and the mixtures preferred were shown in Table 3.

Decalin	solvent A
100%	-
75%	25%
50%	50%
25%	75%
-	100%

Table 3: Compositions of decalin and solvent A used for production of UHMwPE films

2.1.3. Experiment C - variation of alkyl chain length to decrease the solvent quality

[REDACTED]t. This will be later checked with DSC measurements. The schematic representation of this objective is given in Figure 11.

Hence, to explore this hypothesis **linear** chained compounds were used. Firstly, in compounds, as solvent A is already known as non- solvent [36], so the compounds with increasing number of carbon

atoms have chosen so that the polarity decreases and quality improves to make It a bad solvent. The structure of the compounds chosen were shown in Table 4 .

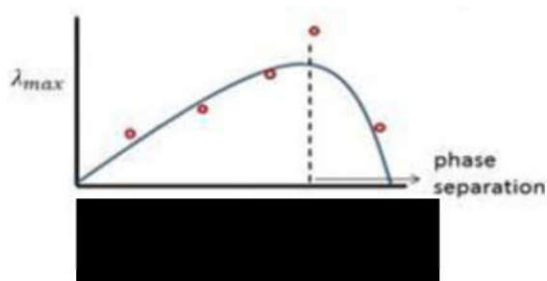


Figure 11: Maximum draw ratio as a function of solvent quality: hypothesis C

Solvent	Structure	Number of carbon atoms
Solvent A		
Solvent B		
Solvent C		

Table 4: Selected solvents by varying the chain length in compounds

As stearic acid was already know as low quality solvent (improving fiber properties drastically) [33], the idea was to choose the

d. The solvents chosen from compounds are given below in Table 5.

Solvent	Structure	Number of carbon atoms
Solvent D		
Solvent E		
Stearic acid		
Solvent F		

Table 5: Selected solvents by varying the chain length

2.2. Methods

This section starts with the explanation of procedure for differential scanning calorimetry which was used to determine the dissolution temperatures of various selected solvents in UHMwPE and also dissolution (flask) experiments. Next, the production of UHMwPE films by gel casting process was explained, followed by solvent removal process from the films, hand drawing procedure of the solvent free films and determination of modulus by using Dynamic Mechanical Thermal Analysis. At the end, procedures of rheology, scanning electron microscope and X-ray diffraction experiments were elucidated which are used to analyze the solvent quality effect.

2.2.1. Differential scanning calorimetry

Differential scanning calorimetry (DSC) is a thermo analytical technique in which the difference in the amount of heat required to increase the temperature of a sample and reference is measured as a function of temperature. The basic principle underlying this technique is that when the sample undergoes a physical transformation such as phase transitions, more or less heat will need to flow to it than the reference to maintain both at the same temperature. By observing the difference in heat flow between the sample and reference, differential scanning calorimeters are able to measure the amount of heat absorbed or released during such transitions. DSC may also be used to observe more subtle physical changes, such as glass transitions. It is widely used in industrial settings as a quality control instrument due to its applicability in evaluating sample purity and for studying polymer curing [34]. Based on the mechanism of operation, DSCs can be classified into two types: heat-flux DSCs and power-compensated DSCs. In a heat flux DSC, the sample material, enclosed in a pan, and an empty reference pan are placed on a thermoelectric disk surrounded by a furnace. The furnace is heated at a linear heating rate, and the heat is transferred to the sample and reference pan through the thermoelectric disk. However, owing to the heat capacity (C_p) of the sample, there would be a temperature difference between the sample and reference pans, which is measured by area thermocouples, and the consequent heat flow is determined by the thermal equivalent of Ohm's law [35]:

$$q = \frac{\Delta T}{R} \quad [8]$$

Where:

- q is sample heat flow
- ΔT is temperature difference between sample and reference
- R is resistance of thermoelectric disk

In a power-compensated DSC, the sample and reference pans are placed in separate furnaces heated by separate heaters. The sample and reference are maintained at the same temperature, and the difference in thermal power required to maintain them at the same temperature is measured and plotted as a function of temperature or time.

In this project, DSC experiments were carried out made in order to study the melting point depression (T_m) of UHMWPE in different solvents. All the experiments were performed in the Q2000 TA Instrument (see Figure 12a), a heat flux DSC, using high pressure pans with gold safety lids. An identical empty pan is used as reference. Nitrogen gas was purged at a rate of 50 ml/min. Heating-cooling-heating cycles in the range from 20°C to 160°C, and a rate of x°C/min were applied. The samples were prepared using a weight of UHMWPE between 0.9-1mg, and based on the concentration of PE (10%) in the solution, the amount of solvent necessary was calculated and then added through the micro-syringe (see Figure 12).



Figure 12: (a) Q2000 TA Instrument: DSC experimental setup (b) preparation of DSC sample in high pressure pan

Here, T_m obtained from DSC experiments were used mainly for two reasons, one is to identify the dissolution temperature for producing UHMWPE films in various selected solvents by gel casting process (Explained in section 2.2.2). The other reason is to experimentally evaluate the quality of the solvents in UHMWPE. As the chi parameter is a measure of solvent quality, according to melting point depression theory, the relation between X and T_m is given by Flory Huggins equation [28] which is;

$$\frac{1}{T_m} - \frac{1}{T_m^0} = \frac{R}{\Delta H_u} \left(\frac{V_u}{V_1} \right) [(1 - v_2) - \chi_1 (1 - v_2)^2] \quad [9]$$

Where:

- T_m is the melting point of the mixture/dissolution
- T_m^0 is the melting pint of pure polymer
- R is the gas constant
- ΔH_u is the heat of fusion of pure polymer
- V_u is the molar volume of repeat unit
- V_1 is the molar volume of the solvent
- v_2 is the polymer volume fraction
- χ_1 is the interaction parameter (chi)

According to Equation 9, the melting point of dissolution depends on the volume fraction of diluents in the mixture, its molar volume and the thermodynamic interaction between polymer and solvent. However, in this project, except T_m , χ_1 and V_1 remaining all the terms will be constant. Thus, for the good solvents ($\downarrow \chi_1$), a melting temperature of dissolution ($\uparrow T_m$) should be observed and vice versa. Nonetheless, the

molar volume (V_1) will also have a significant effect on χ_1 i.e. higher molar volume may also lead to lower χ_1 indicating a good solvent.

2.2.2. Gel casting process

Gel casting process can be used for the production of UHMwPE films in various solvents at different concentrations. In this project, mostly the films are made at 10% w/w. So, in this process, firstly solution is prepared in a metal syringe with 10% UHMwPE and 90% solvent in it. This solution is stirred with spatula and fed into the twin screw extruder (see Figure 13a). Here, it has to be mentioned that some of the solvents are solids/semi-solids at room temperature. So to make a solution before extrusion, the solvent has to be melted. The metal syringe also has to be heated up so that when the solution is mixed in it the solvent doesn't solidify before feeding into the extruder. This extruder is used for mixing, the sample is gradually melted by the mechanical energy generated by rotating twin screws and by heaters around them. The motor speed (screw rotation) of the extruder is x rpm (optimum value) but the temperature of the extruder should be chosen depending upon the melting point of dissolution of the respective solution as shown in Table 5. After x minutes of mixing, the extrudate (gel) is placed in the pre heated rectangular mold (see Figure 13b) by opening the outlet of the extruder. This mold with sample is placed in between the metal plates and pressed under compression mould at x°C as shown in Figure 13c. Here, the gel is pressed to have a consistent and homogenous sample for further experimentation. After x mins in the press, the metal plates are removed and mold is cooled in air, then the film is cut out from the mold (see Figure 15a). Subsequently after the film production, solvent extraction and drawing of the films was carried out.

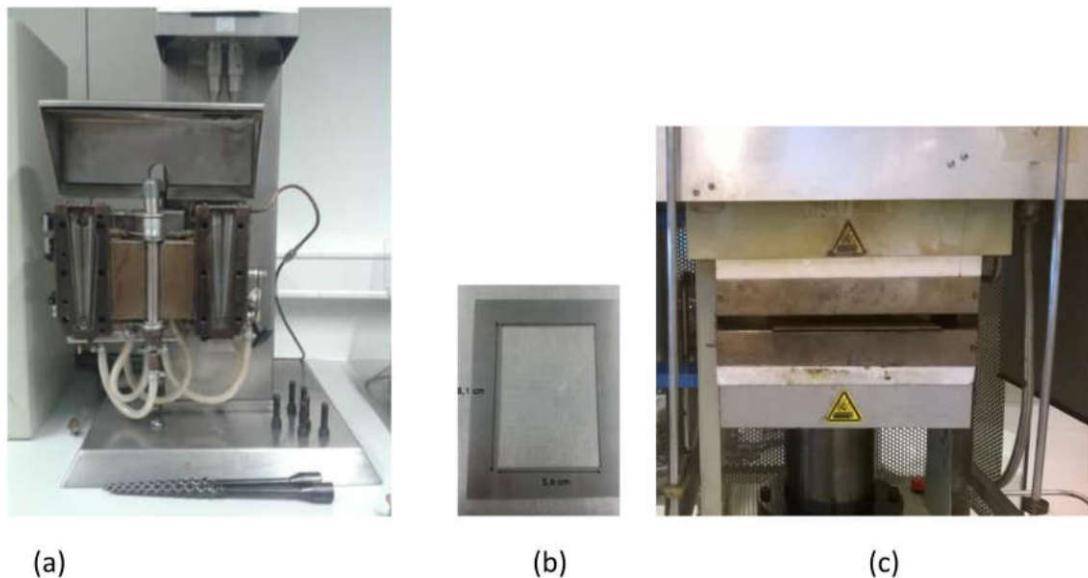


Figure 13: Experimental setup for gel casting process (a) Twin screw extruder, (b) rectangular mold (c) compression press

The approximate quenching rate when the gel casted film cooled in air was x C/sec. The drawing results will be discussed in section 4.2.

Solvent	Melting point of solvent (°C)	T _m (melting point depression of the solution) (°C)	T _{extruder} (°C)
Decalin	- 30.4		
Paraffin oil	-24		
Stearic acid	69		
Solvent A			
Solvent B			
Solvent C			
Solvent D			
Solvent E			
Solvent F			

Table 5: Extrusion temperatures and melting points of the solvents

In Table 5, the melting point depression of different cases were measured from the DSC experiments with 10%polymer/90% solvent (w/w %). The first heating curves of some of the solvents are plotted in Figure 15. The first heating curve of pure UHMwPE was also included to have a relative comparison. In order to validate the DSC results, dissolution experiments in a flask were conducted. Here, 10%polymer/90% solvent is poured in the flask and it is placed inside an oil bath with a magnetic stirrer. The dissolution process was visually observed while gradual increasing the temperature. Once, the dissolution temperature is reached the solution becomes transparent and the corresponding temperature is noted down. It was found that the values obtained from the dissolution experiments were almost in line with DSC experimental results (appendix D).

From Table 5 (blue color), it can be observed that some of the solvents are solids/semi-solids at room temperature, it can be seen in stearic acid case in Figure 15, first the melting of the solvent and then the melting of the solution will take place. The extrusion temperature has been chosen such that it is approximately 70°C above the melting point of PE in solution to ensure the homogeneous mixing and also the formation of gel. One of the other reasons to choose higher extrusion temperature is to avoid the degradation in the midi-extruder, lower the dwell temperature leads to higher torque which may result in mechanical degradation. So, the optimum temperature was chosen as high as possible but also lower than boiling point of solvent to avoid evaporation of solvent which can create differences in concentration.

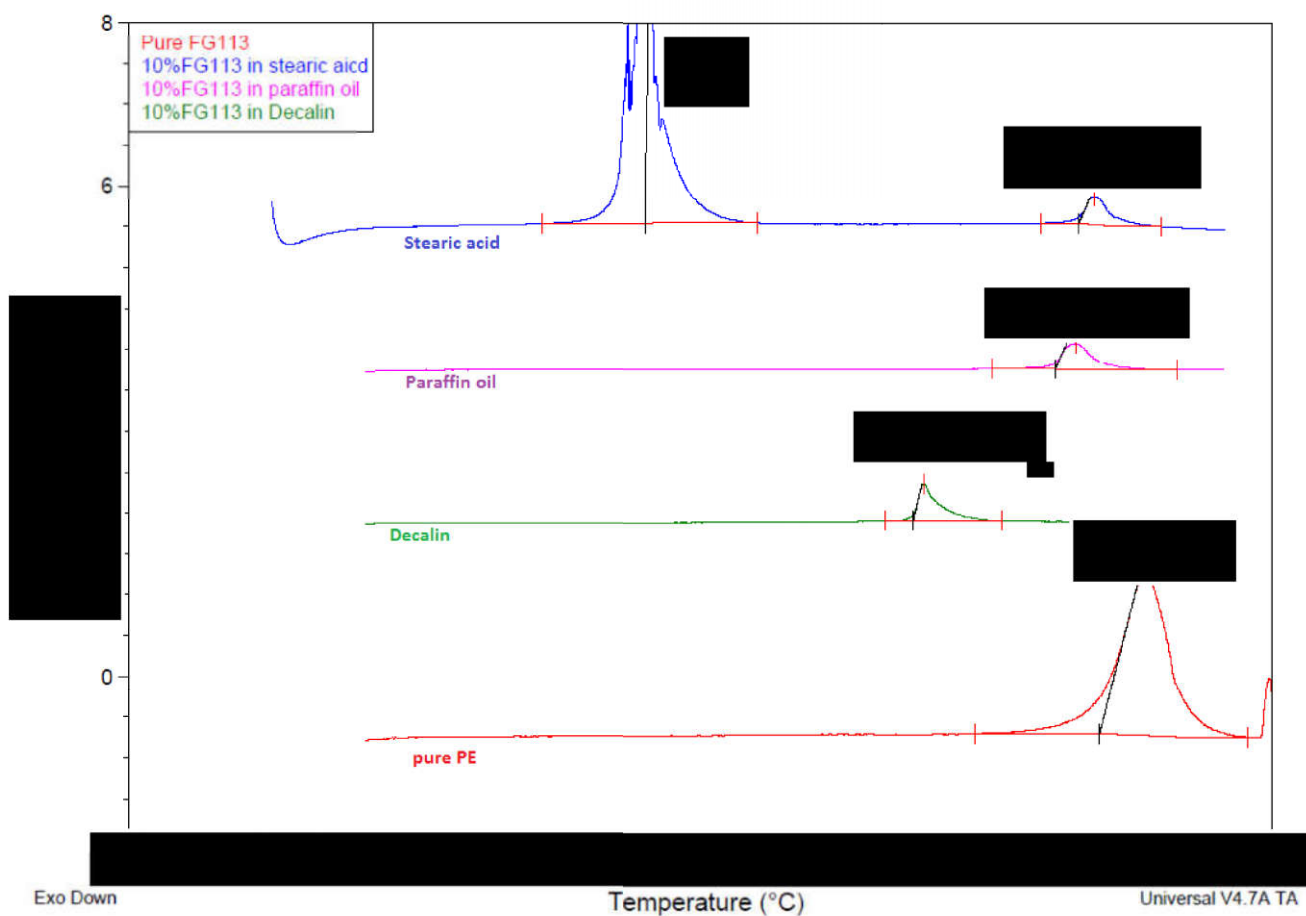


Figure 14: First heating curves of 10% UHMWPE in reference solvents.

2.2.3. Solvent removal process

After the production of the films, next step is to remove the solvent from it. Here, the extraction or evaporation process was used depending upon the volatility and solubility of the solvent. For the films made from volatile solvents, the solvent was removed by evaporation method by simply keeping the film in oven with vacuum and nitrogen flush at a certain temperature. For non-volatile solvents, washing agent was used to extract the solvent. The washing agents used for different solvents and also the procedure is detailed in Table 6.

Solvent	Extraction agent	Process
Decalin	-	Film is placed kept in oven under vacuum at room for x days
Paraffin oil	-	Firstly, the film is kept in washing agent for x days. Then the washing agent is removed by placing the film in vacuum under N ₂ flush.
Stearic acid	-	"
Solvent A	-	Film is placed kept in oven under vacuum for x days
Solvent B	-	Firstly, the film is kept in washing agent for x days. Then the washing agent is removed by placing the film in vacuum under N ₂ flush for x days.
Solvent C	-	"
Solvent D	-	"
Solvent E	-	"
Solvent F	-	"

Table 6: Solvent removal procedures for all the selected solvents

The gel casted films which have to be evaporated are kept in the oven between two metallic plates which is necessary to control the shrinkage that occurs during the evaporation of the solvent predominantly perpendicular to the film causing a reduction of the thickness [26]. For extraction step, initially the container (see Figure 16b) has to be filled with half a liter of respective washing agent and then the film is put into it. After the solvent extraction, the washing agent in the film was removed by keeping it in the oven between two metallic plates. The film after the removal of solvent looks as it is shown in Figure 16c.

In solvent F case, two films were gel casted and extracted with two different solvents. The respective results were presented in section 4.3.



Figure 15: (a) UHMwPE film before solvent removal, (b) grey container used for solvent extraction, (c) solvent free film

2.2.4. Hand drawing process

Hand-drawing tests on the dried films were performed on Kofler hot bench shown in Figure 16. It is a metal strip with a temperature gradient which can be used to hand draw the films with a gradual increase in temperature by moving vertically. To perform hand drawing, firstly from the solvent-free film, a bar of 3mm width is cut carefully with a knife (smooth and sharp surface) and a rubber hammer. If a bad knife is used, the bar will not loosen in a single shot and crack initiation point arise at this location. Hence, the bar should be cut in one shot with a sharp knife. The one centimeter middle part of the cut piece will be marked at 0.2cm of intervals as shown in Figure 17. A well-defined marked was used for good contrast. Then the bar will be clamped at the ends with the help of clamping tools (see in Figure 16). If there is no sufficient gripping between the clamp and bar, the material will slip easily between the clamps destructing the morphology. Some films were extremely porous (appeared white because of scattering) and have measured density 0.2-0.5 g/cm³ instead of expected 0.97 g/cm³ (density of polyethylene). [REDACTED]



Figure 16: Kofler hot-bench used for hand drawing

The ran [REDACTED]

[REDACTED] °C.

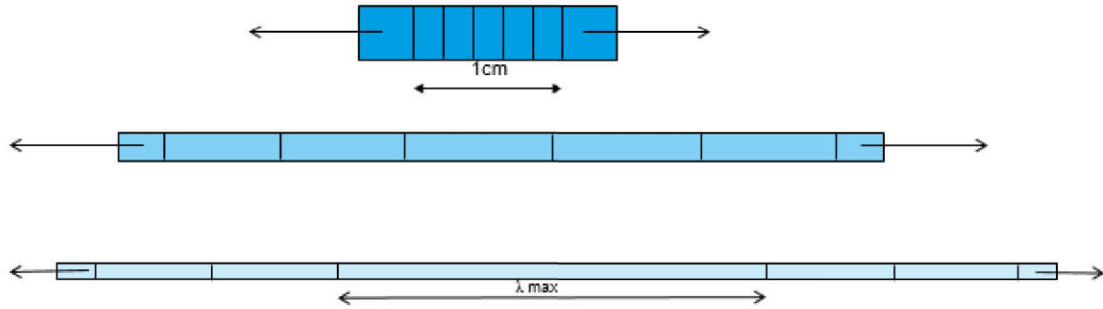


Figure 17: schematic representation of hand-drawing procedure

St [REDACTED]
[REDACTED]
[REDACTED]
[REDACTED]
[REDACTED]
[REDACTED]
[REDACTED]
[REDACTED]
[REDACTED] different objectives will be discussed in section4.

2.2.5. Dynamic Mechanical Thermal Analysis

Dynamic mechanical analysis is useful for studying the viscoelastic behavior of polymers. A sinusoidal stress (equation 10) is applied and the strain (equation 11) in the material is measured, allowing one to determine the complex modulus [37].

$$\sigma = \sigma_0 \sin(\omega t + \delta) \quad [10]$$

$$\varepsilon = \varepsilon_0 \sin(\omega t) \quad [11]$$

Where ω is the frequency of strain oscillation, t is time and δ is phase lag between stress and strain.

For a perfectly elastic solid, the resulting strain and the stress will be perfectly in phase. In this case we have:

$$\sigma(t) = E\varepsilon(t) \Rightarrow \sigma_0 \sin(t\omega + \delta) = E\varepsilon_0 \sin(\omega t) \Rightarrow \delta = 0 \quad [12]$$

For a purely viscous fluid, there will be a 90° phase lag of strain with respect to stress, stress is proportional to strain rate

$$\sigma(t) = K \frac{d\varepsilon}{dt} \Rightarrow \sigma_0 \sin(\omega t + \delta) = K \varepsilon_0 \omega \cos(\omega t) \Rightarrow \delta = \frac{\pi}{2} \quad [13]$$

But for viscoelastic polymers (which is in our case) have the characteristics in between where some phase lag will occur during DMA tests. Here, the storage modulus measures the stored energy, representing the elastic portion and the loss modulus measures the energy dissipated as heat, representing the viscous portion. The tensile storage and loss moduli are defined as follows [37]:

- Storage Modulus: $E' = \frac{\sigma_0}{\varepsilon_0} \cos \delta$ [14]

- Loss Modulus: $E'' = \frac{\sigma_0}{\varepsilon_0} \sin \delta$ [15]

- Phase Angle: $\delta = \arctan \frac{E''}{E'}$ [16]

In this project, DMA was performed to measure the Young's modulus of the films at different draw ratio. To perform this tests, a piece of 4cm in length was cut out of the drawn film. The thickness and width were measured with the calibrated Heidenhain thickness meter and an optical microscope respectively. The dynamic mechanical analyses were carried out using a RSA-G2 (see Figure 18) test system at a frequency of 1 Hz and at a temperature of 30 °C. During the measurements, the storage modulus (E') of the film at a specific draw ratio was determined. Thus, films of different solvents were draw to various draw ratios and respectively Young's modulus values were determined.

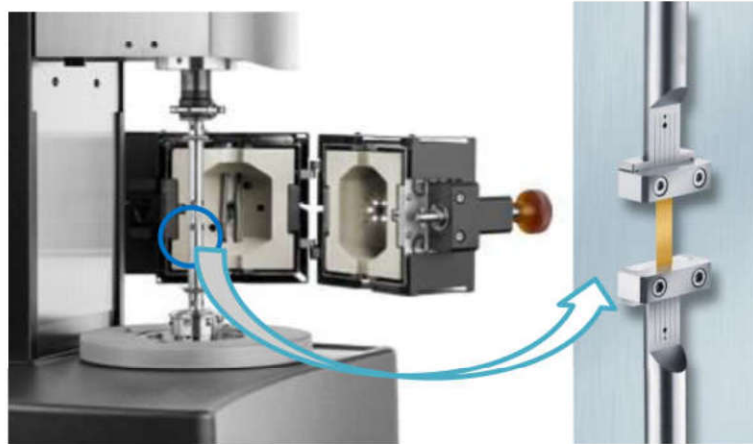


Figure 18: RSA-GS2: DMTA experimental setup

2.2.6. Rheological analysis

2.2.6.1. Methodology [38]

Rheology is the study of the flow of matter: it characterizes the response of matter under an applied stress or strain. The possible behaviors range from purely viscous to purely elastic, going through a whole range of visco-elastic behaviors which are determined by the nature and structure of matter. A rheometer is a laboratory device used to measure the way in which a liquid, suspension or slurry flows in response to

applied stress or strain. It allows a full characterization of fluids which cannot be described by a single value of viscosity (Newtonian fluids) but which show more complex behavior (for example: viscoelastic fluids).

Polyethylene gels are viscoelastic in nature. This means they behave partly like an elastic solid (deformation due to loading is recoverable – it is able to return to its original shape after a load is removed) and partly like a viscous liquid (deformation due to loading is non-recoverable – it cannot return to its original shape after a load is removed). Having been used in the plastics industry for years, the Dynamic Shear Rheometer is capable of quantifying both elastic and viscous properties. This makes it well suited for characterizing polyethylene gels in this project.

A typical experiment to characterize visco-elastic fluids, is an oscillatory experiment, where an oscillatory deformation with a fixed amplitude is applied at different frequencies. The stress response of the fluid is recorded in 2 parameters: complex modulus and phase angle. Both parameters are used to describe the fluid behavior. The complex shear modulus (G^*) can be considered the sample's total resistance to deformation when repeatedly sheared, while the phase angle (δ) is the lag between the applied shear stress and the resulting shear strain as shown in Figure 19. The larger the phase angle (δ), the more viscous the material. Phase angle (δ) limiting values are:

- Purely elastic material: $\delta = 0$ degrees and purely viscous material: $\delta = 90$ degrees

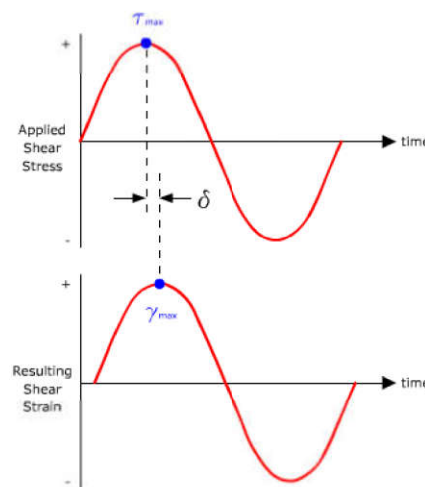


Figure 19: input and output signal of a typical; shear rheology measurement

2.2.6.2. Sample preparation

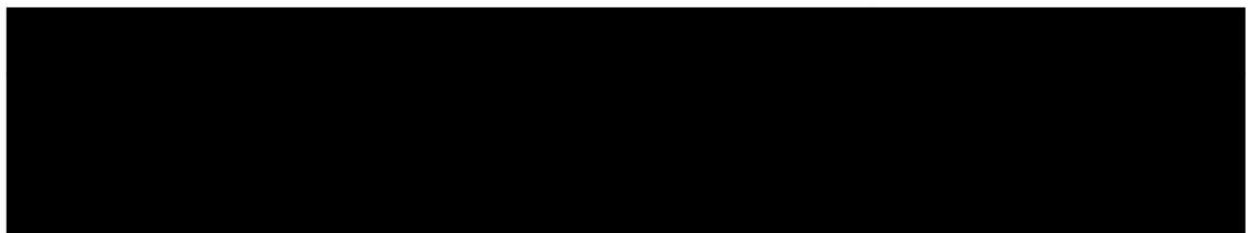




Figure 20: (a) ARES-LS2; schematic representation of shear rheometer, (b) zoom in of the sample holder

2.2.7. Morphological analysis - scanning electron microscope



First let us understand the working of scanning electron microscope (SEM). It is a type of electron microscope that produces images of a sample by scanning it with a focused beam of electrons. The electrons interact with atoms in the sample, producing various signals that contain information about the sample's surface topography and composition [39]. A beam of electrons is produced at the top of the microscope by an electron gun. The electron beam follows a vertical path through the microscope, which

is held within a vacuum. The beam travels through electromagnetic fields and lenses, which focus the beam down toward the sample [40]. A schematic representation is shown below in Figure 21a. Once the beam hits the sample, electrons and X-rays are ejected from the sample, as in Figure 21b. Detectors collect these X-rays, backscattered electrons, and secondary electrons and convert them into a signal that is sent to a screen producing the final image [39].

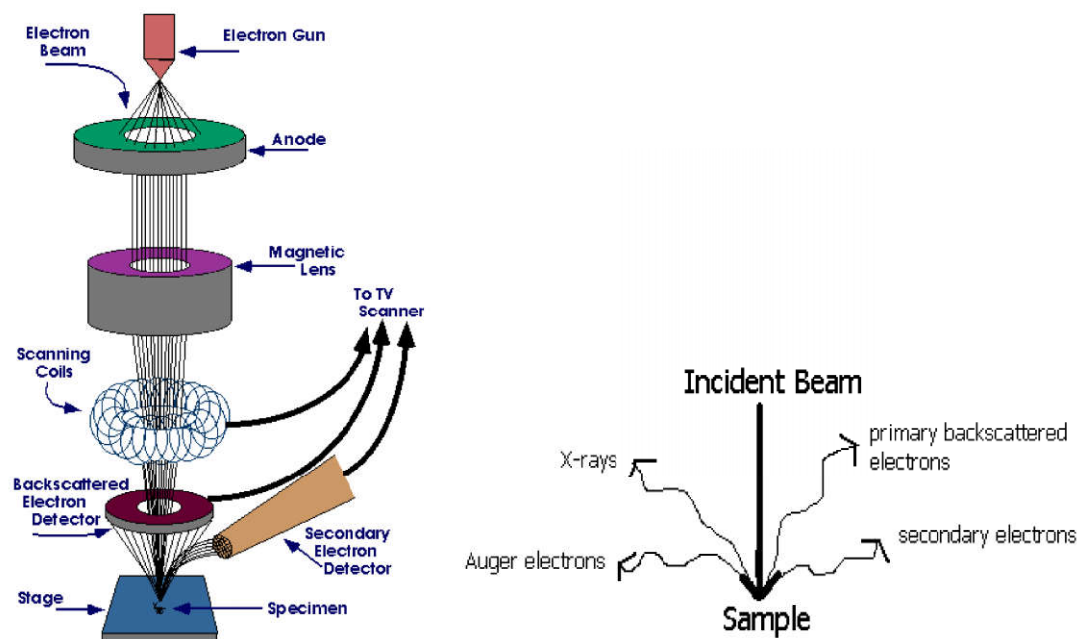


Figure 21: (a) Schematic representation of the SEM components, (b) Interaction between the incident beam of electrons and the sample

In this project, the SEM analysis were performed using Phenom G2 pro. Here cross section of the solvent free films was observed in SEM after breaking it in liquid nitrogen. As the SEM utilizes vacuum conditions and uses electrons to form an image, special preparations must be done to the sample. All the water must be removed from the samples, because the water would vaporize in the vacuum. All non-metal samples need to be made conductive by covering the sample with a thin layer of conductive material. The coater uses an electric field and argon gas. The sample is placed in a small chamber that is in vacuum. Argon gas and an electric field cause an electron to be removed from the argon, making the atoms positively charged. The argon ions then become attracted to a negatively charged gold foil. The argon ions knock the gold atoms from the surface of the gold foil. These gold atoms fall and settle onto the surface of the sample producing a thin gold coating. The coating was performed using Quorum Q 150R S.

2.2.8. Morphological analysis - X-ray diffraction

WAXD (Wide Angle X-ray Diffraction) and SAXS (Small-angle X-ray scattering) are two particular techniques of X-ray diffraction that refer to the analysis of Bragg's peaks. Bragg diffraction occurs when radiation with wavelength comparable to atomic spacing, is scattered in a specular fashion by the atoms of a crystalline system and undergoes a constructive interference. For a crystalline solid, the waves are scattered from lattice planes separated by inter planar distance d . When the scattered waves interfere constructively, they remain in phase since the path length of each wave is equal to an integer multiple of the wavelength [41]. It follows the Bragg's law:

$$\frac{1}{d} = \frac{2 \sin \theta}{n\lambda} \quad [17]$$

Where d the spacing between the planes in the atomic lattice is θ is the angle between the incident ray and the scattering planes, n is a positive integer and λ is the wavelength of incident wave

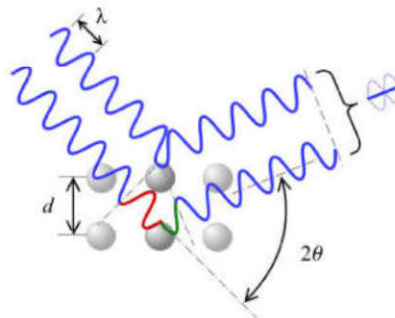


Figure 22: Bragg's diffraction and constructive interference of the incident radiation

The difference between WAXD and SAXS is only the distance from the sample to the detector. For SAXS, it is shorter and thus diffraction maxima at larger angles are observed and vice versa for WAXD. Hence the results obtained from this techniques will be entirely at different length scales. In this project, study

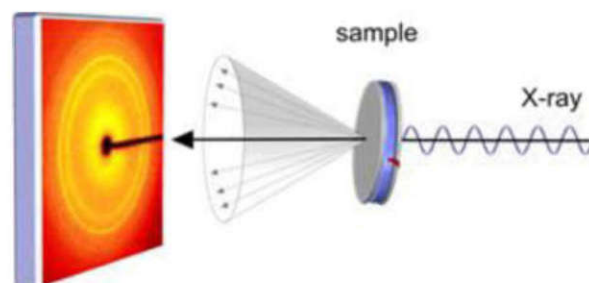


Figure 23: WAXD and SAXS in transmission

WAXS measures the interatomic spacing within the unit cell, for polyethylene it is usually an orthorhombic base-centered unit cell: $a \neq b \neq c$ and $\alpha = \beta = \gamma = 90^\circ$. the interatomic spacing is calculated with the following equation.

$$d = \left[\left(\frac{h^2}{a^2} \right) + \left(\frac{k^2}{b^2} \right) + \left(\frac{l^2}{c^2} \right) \right]^{-\frac{1}{2}} \quad [18]$$

This diffractometric technique allows also to calculate the degree of crystallinity (X_c) that is related to the area under the crystalline and amorphous peaks of the diffractometric pattern. Below a typical pattern for PE with the crystalline peaks (red in Figure 24) and amorphous peak (black in Figure 24).

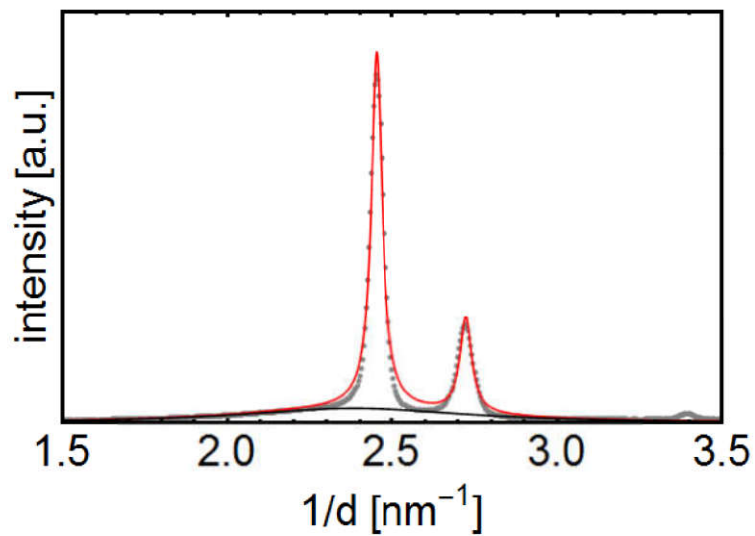


Figure 24: Typical WAXD pattern with the fitting of crystalline and amorphous peaks

3. Materials and Experimental procedures for the production of UHMwPE fibers

3.1. Materials

In the production process of UHMwPE fibers, the polymer used was UHMWPE grade (same as used in gel casting process). The antioxidant (stabilizer) used was x where x% (w/w% based on solvent) was added to the solution. The solvents used in this process were given in Table 7. Here decalin, paraffin oil and stearic acid were chosen to understand the translation of gel casting to solution spinning process. Solvent B was also chosen because the UHMwPE film made solvent B was undrawable, so to understand how this translates to fibers.

Solute	Solvent	Draw down
UHMWPE	Decalin	1
UHMWPE	Paraffin oil	1
UHMWPE	Stearic acid	1
UHMWPE	Solvent B	1

Table 7: Solvents used for solution spinning

Here draw down corresponds to the liquid state drawing i.e. the fiber is drawn (oriented) to some extent during the spinning process itself. Another point to mention is, although in commercial process, the fibers are produced without using the stabilizer to achieve higher draw ratios (absence of stabilizer will lead to have short chains which makes the drawing comparatively easy) but here, we choose to use stabilizer in the sample preparation because to eliminate the effect of degradation which will vary depending upon the solvent. Even though, the achievable draw ratios will be relatively less but the effect of degradation will be neutralized with the addition of stabilizer.

3.2. Methods

3.2.1. Solution spinning process

A custom build setup was used for solution spinning of UHMwPE fibers, see Figure 27. The down-scaled laboratory setup allows spinning of only a single fiber instead of several hundred simultaneously as done in the actual commercial process. The fibers were produced at different extruder temperatures (from Table 5) depending upon the solvent used. The detailed process of producing fibers is explained below.

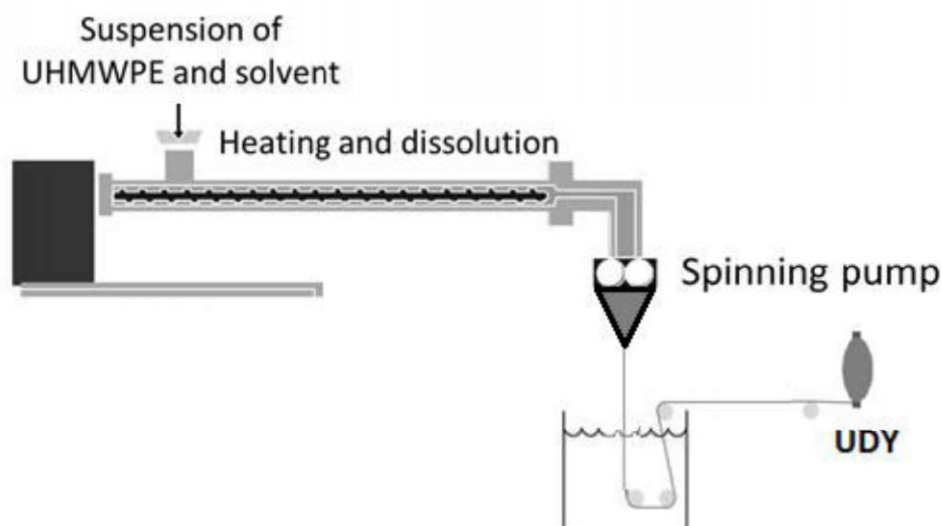


Figure 26: Schematic representation of pilot gel-spinning process.

In the gel-spinning process, a suspension of UHMWPE powder [REDACTED] in a solvent with x % x is fed to an extruder that dissolves the UHMWPE powder by heating it. The solution is effectively mixed in the twin screw extruder (x mm) at a spinning rate of x cc/min. Then this solution is pushed through a small conical die to obtain an elongation flow field that extends the polymer chains. The fiber is pulled out from the die. The fiber formation can be established by enforcing UHMWPE crystallization by quenching in water. Depending upon the required draw down, the difference in V_{out} (the velocity at which the fiber is pulled out from the conical die) and windup speed (the velocity at which the fiber is wound to wooden bobbin) is adjusted. The obtained fiber after cooling is subjected to solvent removal (by evaporation or extraction depending upon the solvent) although partial solvent removal occurs in the air gap during the quench bath (water). Finally, the dry fiber is subjected to extensive hot-drawing for producing filaments.

3.2.2. Solvent removal process

After the production of fibers, the solvent must be removed from the fibers in order to proceed for solid state drawing. As decalin and solvent B are relatively volatile solvents, evaporation method is used to remove the solvent. For paraffin oil and stearic acid respective washing agents are used as mentioned in Table 10.

Solvent	Extraction agent	Process
Decalin	-	Fiber wounded bobbin is placed under vacuum at room temperature for x days
Solvent B	-	
Paraffin oil	-	Firstly, the fiber wounded bobbin is dipped in washing agent for x days. Then the washing agent is removed by placing the bobbin in vacuum under N ₂ flush for x days.
Stearic acid	-	Firstly, the fiber wounded bobbin is dipped in washing agent for x days. Then the washing agent is removed by placing the bobbin in vacuum under N ₂ flush for x days.

Table 8: Solvent extraction procedure for the selected solvents.

3.2.3. Solid state drawing

After the extraction process, fibers were drawn in a tube oven with a length of x m, which is heated by oil. The oven consists of a double cylindrical tube. In the inner tube, the stretching of the fiber occurs and the heated oil flows through the outside tube. The draw-ratio and the draw speed can be regulated with the two motors at both ends of the oven, this is done by adjusting the speed at which the motors turn. During drawing, the diameter of the fiber is measured with an OFDA (Optical Fiber Diameter Analyzer). These devices measure the diameter of the fiber at three different angles at an increments of 60 degree with each other, because the cross section of the fiber is not always circular. The force on the fiber is measured with a load cell, and a personal computer is used to control the temperature of the oil bath, the rotation direction and the velocity of the motors.

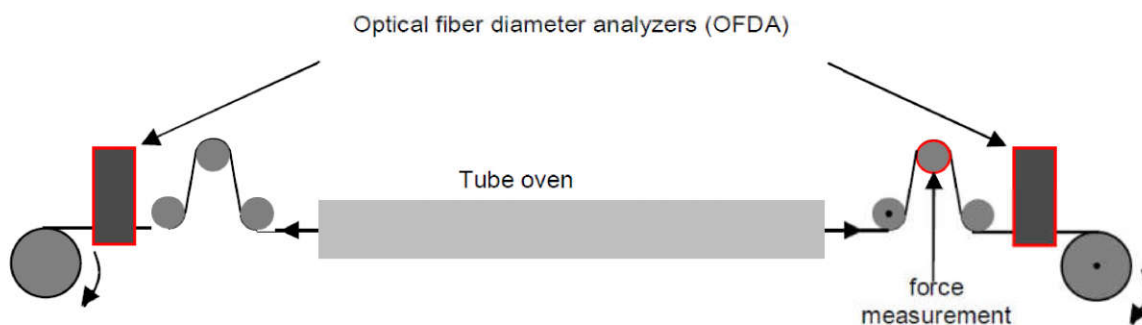


Figure 27: Schematic representation of the drawing oven

4. Results and discussion of UHMwPE films

4.1. Experiment A - effect of solvent quality on the drawability

10% UHMwPE films in decalin, paraffin oil and stearic acid were produced and solvent was removed from them. The subsequent hand drawing results were shown in Figure 29.

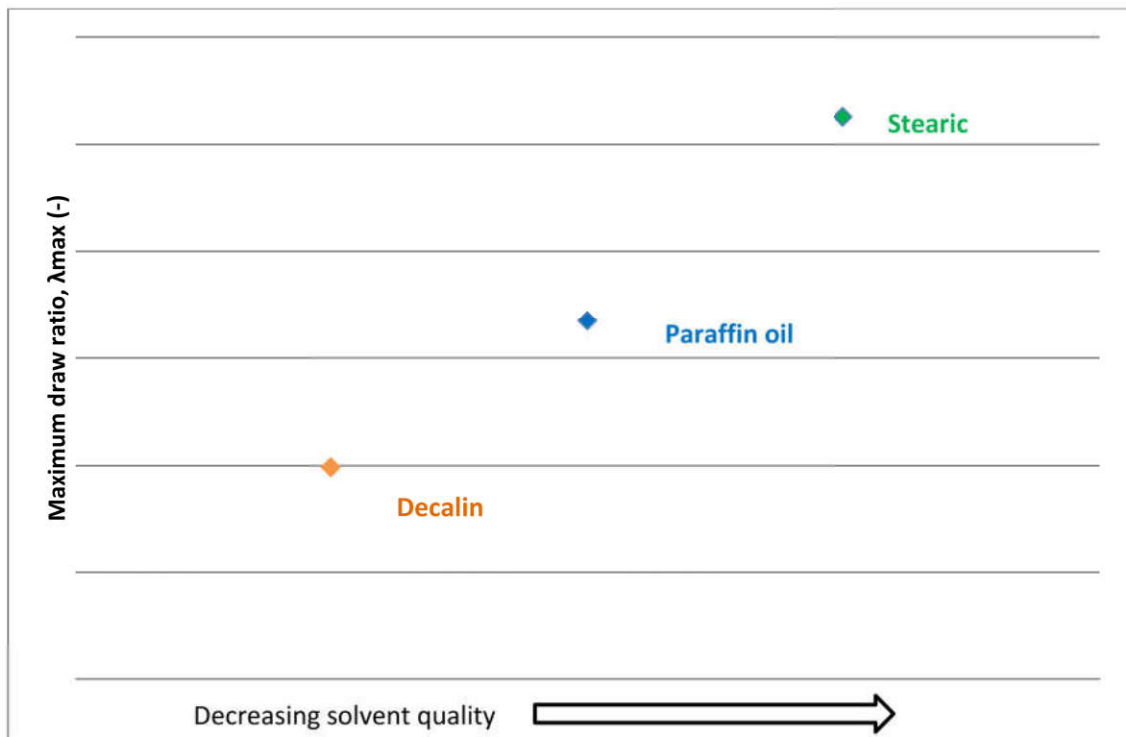


Figure 28: hand drawing results of UHMwPE films in reference solvents

It was found that the maximum draw ratios of decalin, paraffin oil and stearic acid films were [REDACTED]. It is clearly visible that decrease in the solvent quality have a significant impact on the maximum achievable draw ratio of the films. Similar trend was observed by Tervoort et al. [33]: the maximum attainable draw ratio is inversely proportional to the quality of the solvent used. However, due to use of different polymer grades, process steps the explicit values are not achievable. In fact, λ_{max} values in this project were higher than from literature [33].

It was observed that the films produced from cooling procedure2 have higher λ_{max} than that of cooling procedure 1. It was also noticed that the samples were quite homogeneous in cooling condition 2. Although the improvement in λ_{max} of stearic acid film is relatively less when compared with decalin film in this case, the effect of solvent quality on the drawability is still clearly visible.

4.2. Experiment B - blends of a good solvent and non-solvent to vary the solvent quality

The films with blends of solvent A and decalin of difference proportions were quench made. Then the solvent was extracted from these films and later hand drawing tests were performed on them. The results were plotted in the Figure 31.

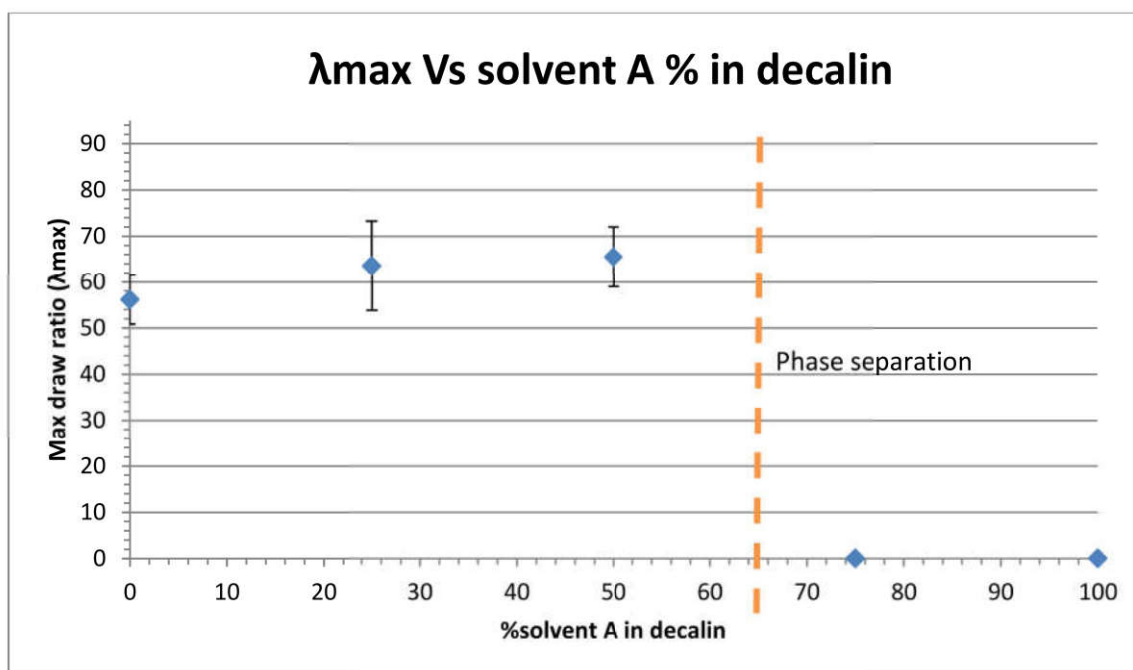


Figure 29: Hand drawing results of UHMwPE films made with decalin/solvent A blends

The maximum draw ratios as a function of solvent A (non-solvent) percentage in decalin was plotted in Figure 32. It was observed that blends of 25% and 50% solvent A were drawable but 75% solvent A blend was undrawable implying that this mixture as a poor solvent and of course pure solvent A film was also not drawable since it is a non-solvent. From this results, we can say that liquid-liquid phase separation occurs somewhere in between 50% and 75% case. This phase separation can be seen from the SEM analysis shown in Figure 33.

However on the other side, it was clearly visible that the increase in draw ratio with these mixtures is slightest when compared to pure decalin case (0% solvent A case from the Figure 31). Thus, the presence of 1-solvent A has only a slight influence on the maximum draw ratio.

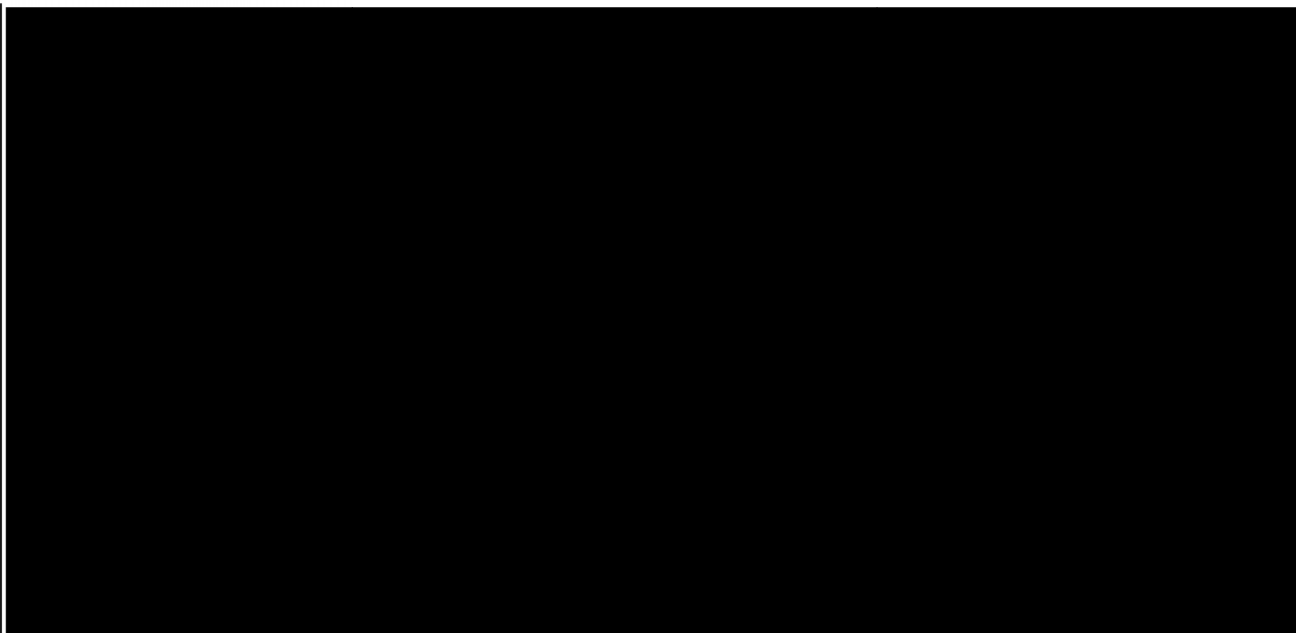
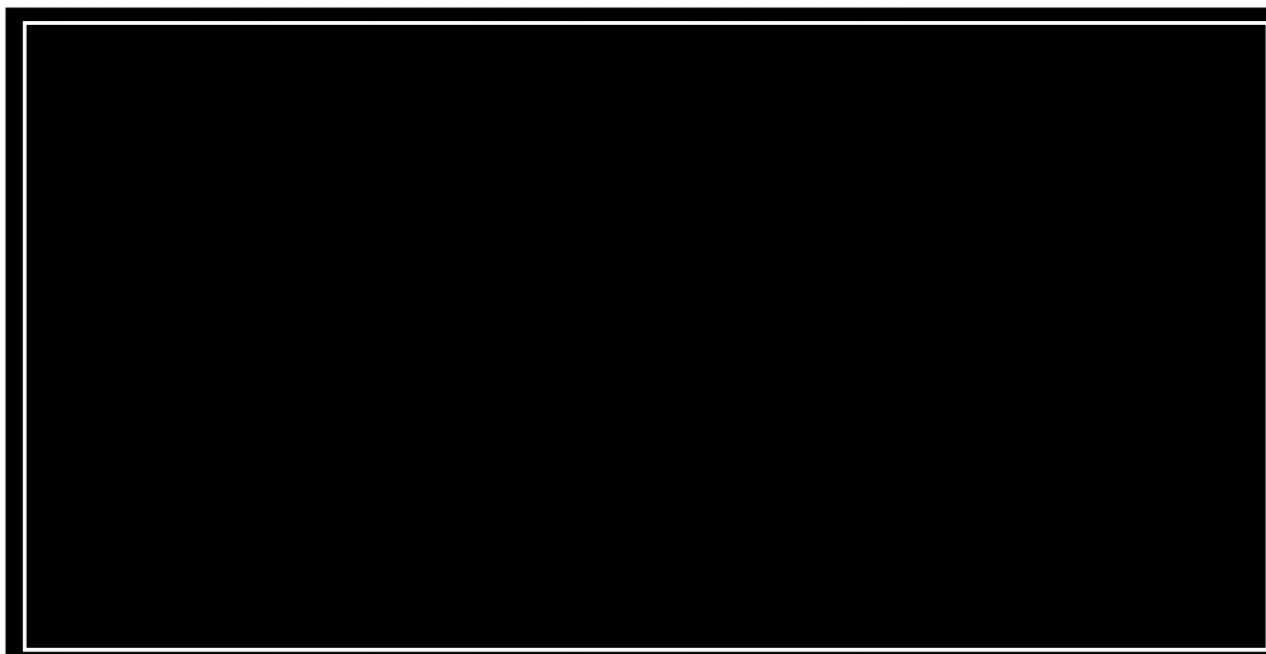


Figure 32 and 33, are the SEM pictures in the cross section of UHMWPE films (after the solvent extraction) which are made from different blend compositions of decalin and solvent A. Here, all the pictures are captured at same magnification. Firstly, if we observe the pictures from Figure 33, the phase separation is clearly visible in these films (75% and 100% solvent A cases), as the PE particles agglomerates and forms globules here and there randomly. The visible empty spot are the solvent occupied space, thus after the solvent extracted, the voids are left behind. T

mixtures. As a result, these samples are drawable but not significantly higher than pure decalin film.



4.3. Experiment C - variation of alkyl chain length to decrease the solvent quality

[REDACTED], films with solvent C and solvent B were quench made, then the solvent was extracted by respective washing agents as shown in section 2.2.3. The hand drawing results of these films were shown in Figure 34 below.

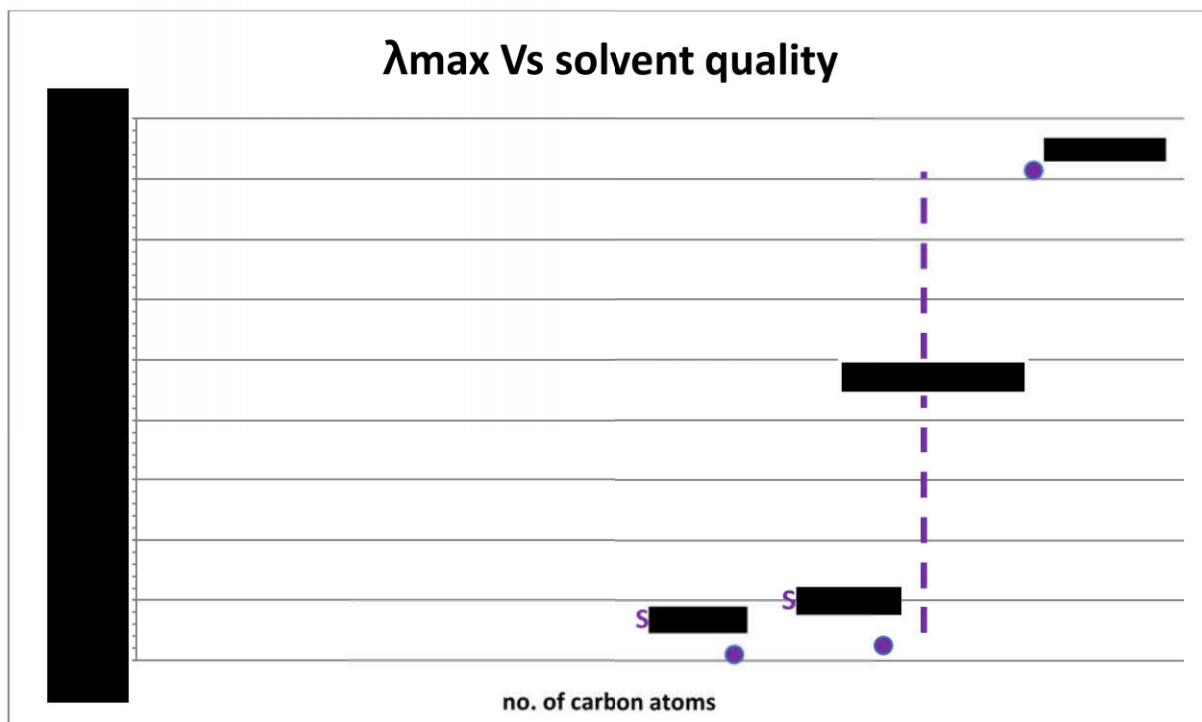


Figure 32: hand drawing results of UHMwPE films made with various selected compounds

The Figure 34 shows the maximum draw ratio as a function of no of carbon atoms along the chain in the chosen compounds, [REDACTED]

[REDACTED] This solvent quality variation was not seen from DSC measurements as it was insensitive for poor solvents. [REDACTED]

[REDACTED] So that drawable UHMwPE films can be made from these obtained new solvents.

Thus, solvent B was chosen initially to produce the UHMwPE film, here the maximum draw ratio was found to be around 2.5 which is still can consider as undrawable indicating that we are still in non-solvent range. Further, solvent C was used to produce the film, and the λ_{\max} turned out to be 81.5, which is relatively higher than the value in decalin case (λ_{\max} 63). Solvent C can be the potential replacement for decalin,

Solvent	Tm1 from DSC measurements (°C)
Stearic acid	-
Solvent E	-
Solvent D	-
Solvent F	-

Table 9: DSC results of different UHMwPE solutions

Here, Tm1 should be inversely proportional to the solvent quality. It is clear all the above mentioned solvents are relative poor in quality when compared to decalin (Tm1 is 111°C). However, due to the insensitivity of DSC measurements at lower solubility, the difference (Tm1's) in between the above mentioned solvents was not clearly visible.

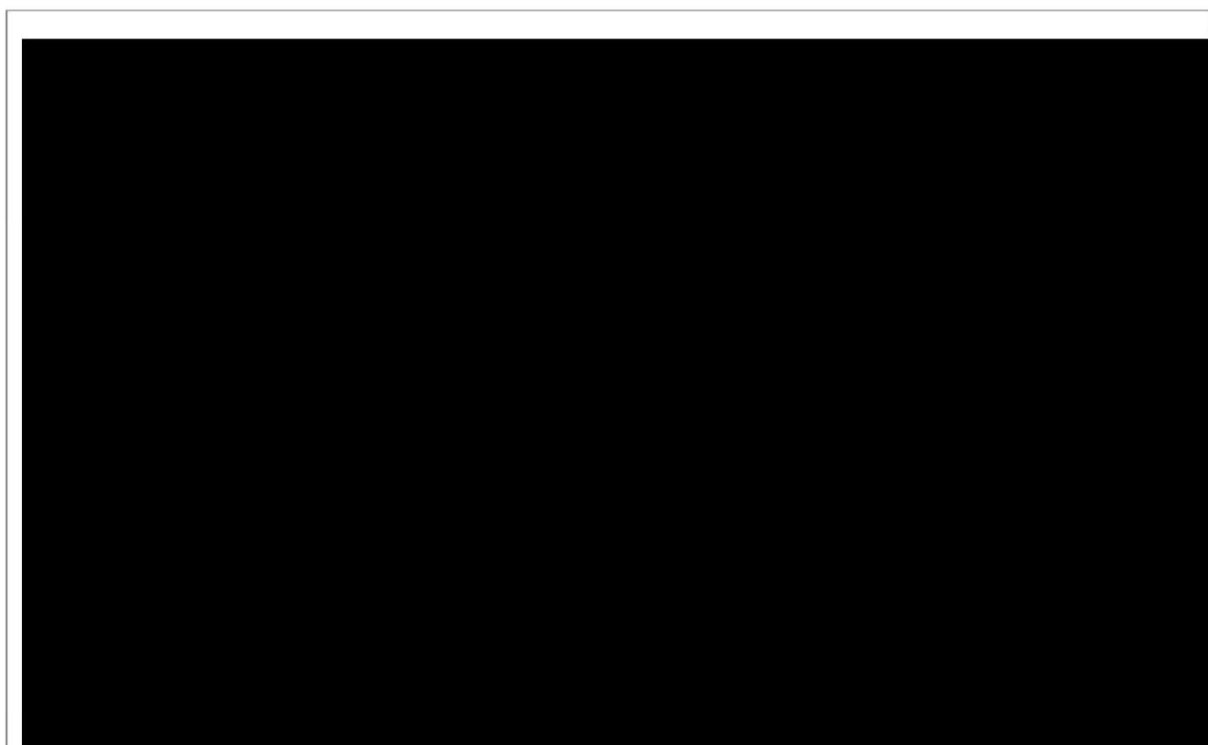


Figure 33: hand drawing results of UHMwPE films made with various selected solvent

Figure 35 shows the hand drawing results of above mentioned solvents. [REDACTED] film as it was undrawable. For solvent E film the obtained λ_{max} was almost similar to that stearic acid case. [REDACTED]. The melting points of both the solvents were already shown in Table 5.

4.4. Mechanical properties

It is essential that the modulus is a unique function of λ_{\max} ; if the properties build up is slowed down in poorer solvents, all the commercial interest might be inadequate. Thus, the aim was to measure the storage modulus (E') of the films produced in different solvents. For this purpose, the films were drawn to different draw ratios (without breaking) and tested on DMTA. The test procedure is already mentioned in section 2.2.5. It should be noted that the storage modulus was measured considering the initial volume, but due to high porosities the modulus values can be corrected by;

$$E'_{\text{corrected}} = E'_{\text{measured}} (0.97/\rho) \quad [19]$$

Here 0.97g/cm³ is the density of poly ethylene and ρ is the density of the specific tape measured. So before testing the tapes, the length, breadth, width and weight of the samples were calculated to estimate the density of that specific tape. Thus the corrected moduli of the films at different draw ratios made from different solvents at different conditions were plotted in Figure 36.

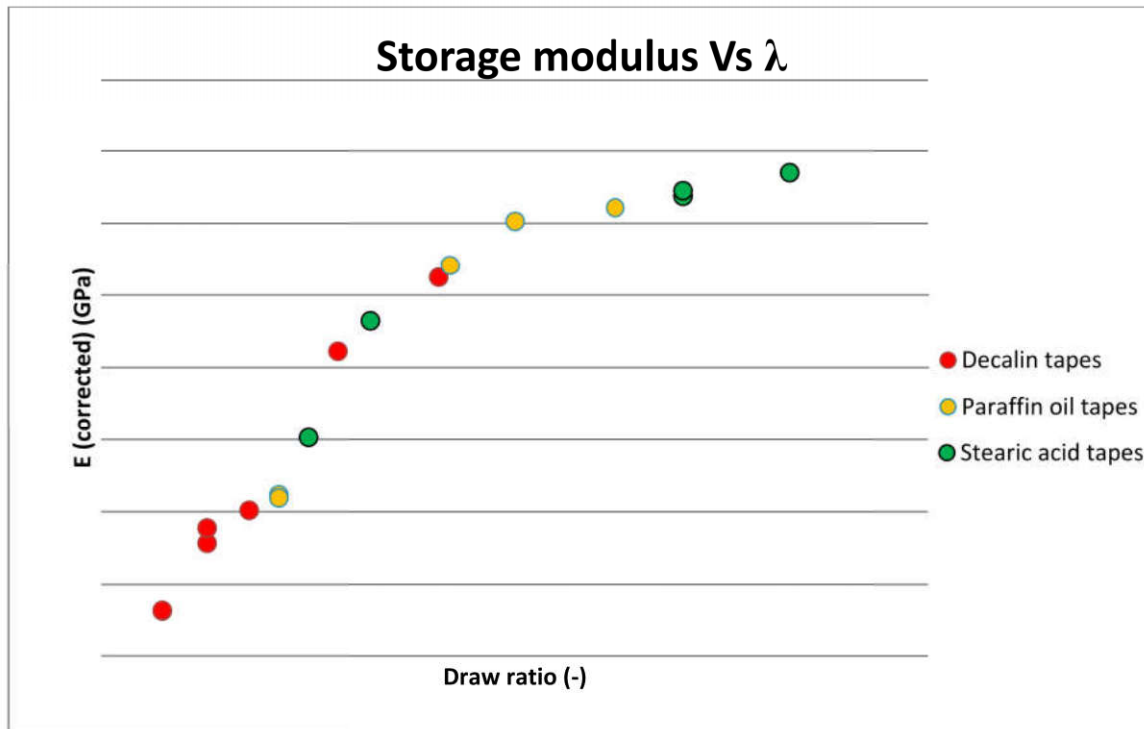


Figure 34: Storage modulus as a function of draw ratio for different solvents

From the above Figure 36, it can be observed that irrespective of the solvent used, the storage modulus is directly proportional to the draw ratio at which it is measured which in line with literature results shown in Figure 8. Thus, it can be concluded that irrespective of the solvent used, the maximum attainable draw ratio dictates the mechanical properties (storage modulus and tensile strength) of the UHMwPE films.

5. Results and discussion of UHMwPE fibers

5.1. Drawing results

[REDACTED]

Table 10: the draw ratios of fibers produced in decalin, PO, SA and solvent B at draw down 1



Figure 35: Drawing force vs time at draw ratio 5 when drawn from UDY to PDY

Al

2).

5.2. Chain kinetics

Since there was no difference in drawability of fibers which is contrary to gel casted films, it was determined to study the impact of different solvents on the chain kinetics during drawing. As there is no direct parameter to measure these kinetics, it should be quantified through the drawing stress. Thus in this scenario, we utilize the stress generated during drawing as a parameter to make relative comparisons between the chain kinetics of UHMWPE fibers in different solvents. During the drawing operation the instantaneous force and diameter of the filament (outgoing part) should be measured at a frequency of 2 Hz. But unfortunately OFDA was not working, so the diameter was estimated. With this data, it is possible to calculate the instantaneous drawing stress during the operation. The respective formulae to obtain drawing stress were given below.

As the capillary diameter through which the fiber was spun is 0.8mm, so the diameter (d_{wet}) of the spun fiber should be the same, from this the diameter (d_{dry}) of the fiber after solvent extraction will be:

$$d_{dry} = d_{wet} * \sqrt{\phi} \quad [27]$$

Here ϕ is the concentration of PE, which is always 10.5% in our case.

From the obtained d_{dry} from above equation 27, the diameter at a specific draw ratio can be calculated by:

$$d_{DR} = \frac{d_{dry}}{\sqrt{DR}} \quad [28]$$

Here DR is the draw ratio and d_{DR} is diameter at that specific draw ratio and DR is the draw ratio of the fiber.

Therefore, the drawing stress (σ) is simply calculated from the equation:

$$\sigma = \frac{F}{\pi * r^2} \quad [29]$$

[REDACTED] S

[REDACTED]

[REDACTED]

[REDACTED]

[REDACTED]

[REDACTED]

[REDACTED]

[REDACTED] S.



Figure 36: Comparison of drawing stresses between stabilized (decalin, PO) and non-stabilized (decalin) fibers

[REDACTED]

[REDACTED]

[REDACTED]

[REDACTED]

[REDACTED]

[REDACTED]

[REDACTED] tions.

6. Conclusions and Recommendations

This research was conducted to understand the effect of solvent quality on the drawability of UHMWPE films, based on literature studies [32, 33]. An emphasis was given to comprehend the effect of solvent quality on the drawing behavior of films and suitable explanations for the experimental observations was provided. Furthermore in second part, preliminary understanding of drawability/chain kinetics of fibers spun in different solvents with the solvent quality was evaluated.

In first part of the thesis, maximum achievable draw ratios of UHMWPE films made from reference (literature) solvents (i.e. decalin, paraffin oil and stearic acid) were evaluated. The appropriate experimental conditions to produce UHMwPE films were determined. From the produced films, solvent was extracted and hand drawing tests were carried out successively. It was found that at cooling condition1 and cooling2 condition, literature results from Tervoort [33] are well reproducible, it was proved that decrease in the solvent quality (from good towards the theta solvent) has a positive impact on the drawability of UHMWPE films. The maximum draw ratio in stearic acid case [REDACTED]

[REDACTED] The Dynamic Mechanical Analysis on the UHMwPE films proved that the final mechanical properties are independent of the solvent used, but only the maximum draw ratio is the controlling factor. Then to quantify this effect of solvent quality on the observed

[REDACTED]

Simultaneously in order to further study the influence of solvent quality on the drawability, it was tried to

[REDACTED]

75%decalin +25%solvent A and 50%decalin +50%solvent A were drawable but the achievable maximum draw ratios were similar to that of decalin (much lower than stearic acid) and in the other blends 25%decalin +75%solvent A and 100% solvent [REDACTED]

[REDACTED] Morphological study through SEM were not able to show an appreciable differences in structure between the drawable samples. Nevertheless, [REDACTED]

[REDACTED] behavior.

[REDACTED]

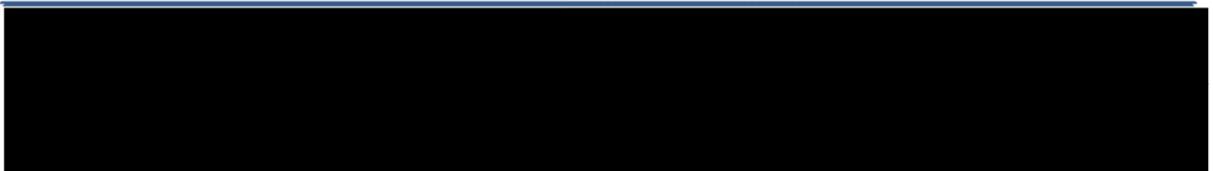
different solvents. However, from Differential Scanning Calorimetry (DSC), it was possible to relate the

melting point depression (T_m) of UHMWPE in solutions to the quality of the solvents used, but in the region of less solubility T_m was insensitive: for approximately same T_m , huge difference in drawability. A possible explanation could be that the cloud point was greater than the crystallization temperature of the polymer in the solvent ($T_{cp} > T_c$) and so the polymer precipitates before crystallizes inducing liquid-liquid phase separation.



The results obtained in this thesis have raised a number of questions, which require further study. The recommendations are as follows:

- Neutron scattering can be conducted to obtain the size of the coils in different solvents.
- In compounds, it was found that films made with solvent B was undrawable [REDACTED] [REDACTED] also [REDACTED]
[REDACTED]
[REDACTED]
[REDACTED]
[REDACTED]



to explicitly understand the spinning process.

- [REDACTED]
[REDACTED]
[REDACTED]
[REDACTED]
[REDACTED]
[REDACTED]
[REDACTED]
- Transmission electron microscope (TEM) analysis on the spun fibers to understand the topology.

7. References

- 1) Barham, L. P., & Keller, A. (1985). High-strength polyethylene fibers from solution and gel spinning. *Journal of materials science*, 20(7), 2281-2302.
- 2) Pennings, A. J., Van Der Hooft, R. J., Postema, A. R., Hoogsteen, W., & Ten Brinke, G. (1986). High-speed gel-spinning of ultra-high molecular weight polyethylene. *Polymer Bulletin*, 16(2-3), 167-174.
- 3) Uehara, H., Yamazaki, Y., & Kanamoto, T. (1996). Tensile properties of highly syndiotactic polypropylene. *Polymer*, 37(1), 57-64.
- 4) Smith, P., & Lemstra, P. J. (1979). Ultrahigh-strength polyethylene filaments by solution spinning/drawing, 2. Influence of solvent on the drawability. *Die Makromolekulare Chemie*, 180(12), 2983-2986.
- 5) Van der Vegt A.K., Govaert L.E. (2003). *Polymeren van keten tot kunststof* (pp.11). DUP Blue Print, Delft.
- 6) Allcock, H. R., Lampe, F. W., Mark, J. E., & Allcock, H. R. (2003). *Contemporary polymer chemistry* (pp. 546). Upper Saddle River, N. J: Pearson/Prentice Hall.
- 7) The Editors of Encyclopedia Britannica. (n.d.). Polyethylene (PE). Retrieved February 07, 2016, from <http://www.britannica.com/science/polyethylene>.
- 8) Doi, M. (1996). *Introduction to polymer physics* (pp. 9). Oxford: Clarendon Press.
- 9) All-Science-of-Plastics | Chemical Heritage Foundation. (n.d.). Retrieved March 15, 2016, from <http://www.chemheritage.org/discover/online-resources/conflicts-in-chemistry/the-case-of-plastics/all-science-of-plastics.aspx>
- 10) Hearle, J. W., Hollick, L., & Wilson, D. K. (2001). *Yarn texturing technology*. Elsevier.
- 11) H. K. C. P. L. Berger, "structure and deformation mechanisms in UHMWPE fibers," *Polymer*, **2003**, vol. 44, pp. 5877-5844.
- 12) Smith P, Lemstra PJ, Booij HC. *J Polym Sci: Polym Phys Ed* **1981**;19: 877.
- 13) Ward, I. M. (1974). Mechanical properties of oriented polymers. *Polymer*, 15(6), 379-386.
- 14) Capaccio, G., Crompton, T. A., & Ward, I. M. (1976). The drawing behavior of linear polyethylene. I. Rate of drawing as a function of polymer molecular weight and initial thermal treatment. *Journal of Polymer Science: Polymer Physics Edition*, 14(9), 1641-1658.
- 15) Bassett, D. C., Keller, A., & Mitsuhashi, S. (1963). New features in polymer crystal growth from concentrated solutions. *Journal of Polymer Science Part A: General Papers*, 1(2), 763-788.
- 16) Keller, A., & Odell, J. A. (1985). The extensibility of macromolecules in solution; a new focus for macromolecular science. *Colloid and Polymer Science*, 263(3), 181-201.
- 17) Dijkstra, D. J., & Pennings, A. J. (1987). Cross-linking of ultra-high strength polyethylene fibers by means of electron beam irradiation. *Polymer Bulletin*, 17(6), 507-513.
- 18) Lemstra, P. J., Van Aerle, N. A. J. M., & Bastiaansen, C. W. M. (1987). Chain-extended polyethylene. *Polymer journal*, 19(1), 85-98.
- 19) Ohta, Y., Murase, H., & Hashimoto, T. (2010). Structural development of ultra-high strength polyethylene fibers: Transformation from kebabs to shishs through hot-drawing process of gel-spun fibers. *Journal of Polymer Science Part B: Polymer Physics*, 48(17), 1861-1872.
- 20) Ohta, O.; Murase, H.; Hashimoto, T. *J. Polym. Sci. Part B Polym. Phys.* **2010**, 48, 1861–1872.

- 21) Smith, P. (1983). Entanglement concepts and drawing of polyethylene. *Macromolecules*, 16(11), 1802-1803.
- 22) Penning J.P. *structure properties relationships in polymeric fibers*. Ph.D. thesis, university of Groningen (1994), 1
- 23) Uehara, H., Yamazaki, Y., & Kanamoto, T. (1996). Tensile properties of highly syndiotactic polypropylene. *Polymer*, 37(1), 57-64.
- 24) Smith, P., & Lemstra, P. J. (1979). Ultrahigh-strength polyethylene filaments by solution spinning/drawing, 2. Influence of solvent on the drawability. *Die Makromolekulare Chemie*, 180(12), 2983-2986.
- 25) Smith, P., & Lemstra, P. J. (1984). *U.S. Patent No. 4,430,383*. Washington, DC: U.S. Patent and Trademark Office.
- 26) Smith, P. (1983). Entanglement concepts and drawing of polyethylene. *Macromolecules*, 16(11), 1802-1803.
- 27) Wagner, Herman L. "The Mark-Houwink-Sakurada equation for the viscosity of linear polyethylene." *Journal of Physical and Chemical Reference Data* 14.2 (1985): 611-617.
- 28) Young, Nicholas P., and Nitash P. Balsara. "Flory-Huggins Equation." *Encyclopedia of Polymeric Nanomaterials* (2015): 777-782.
- 29) <http://www.pslc.ws/macrog/ps5.htm>
- 30) Klein, J. "The onset of entangled behavior in semi-dilute and concentrated polymer solutions." *Macromolecules* 11.5 (1978): 852-858.
- 31) Rajput, A. W., & Arain, F. A. (2014). An Environmentally Friendly Process for the Preparation of UHMWPE As-Spun Fibres. *International Journal of Polymer Science*, 2014.
- 32) Motooka, M., Mantoku, H., Yagi, K., Takeda, H., & Takimoto, K. (1991). *U.S. Patent No. 5,055,248*. Washington, DC: U.S. Patent and Trademark Office.
- 33) Polyethylene Fibers "Al Dente": Improved Gel-Spinning of Ultrahigh Molecular Weight Polyethylene Using Vegetable Oils. *Macromolecules*, 48(24), 8877-8884.
- 34) Leo Mandelkern, *Crystallization of Polymers Volume 1_ Equilibrium Concepts*, Cambridge University Press (2002)
- 35) Gill, P. S., S. R. Sauerbrunn, and M. Reading. "Modulated differential scanning calorimetry." *Journal of thermal analysis* 40.3 (1993): 931-939.
- 36) Boom, R. M., et al. "Linearized cloud point curve correlation for ternary systems consisting of one polymer, one solvent and one non-solvent." *Polymer* 34.11 (1993): 2348-2356.
- 37) https://en.wikipedia.org/wiki/Dynamic_mechanical_analysis
- 38) Doi, Yoshiharu, et al. "Rheology: principles, measurements, and applications." (1994).
- 39) https://en.wikipedia.org/wiki/Scanning_electron_microscope
- 40) <https://www.purdue.edu/ehps/rem/rs/sem.htm>
- 41) Beth A. Miller-Chou, Jack L. Koenig, *A review of polymer dissolution*, Prog. Polym. Sci. 28 (2003) 1223-1270, www.elsevier.com/locate/ppolysci
- 42) https://en.wikipedia.org/wiki/Differential_scanning_calorimetry
- 43) Larson, R. G. (1999). *The structure and rheology of complex fluids* (Vol. 150). New York: Oxford university press.

- 44) Clasen, C., Plog, J. P., Kulicke, W. M., Owens, M., Macosko, C., Scriven, L. E., & McKinley, G. H. (2006). How dilute are dilute solutions in extensional flows? *Journal of Rheology (1978-present)*, 50(6), 849-881.
- 45) De Boer, J. H. "The influence of van der Waals' forces and primary bonds on binding energy, strength and orientation, with special reference to some artificial resins." *Transactions of the Faraday Society* 32 (1936): 10-37.
- 46) Bastiaansen, C. W. M. PhD. Thesis, Eindhoven University of Technology, 1991.
- 47) <http://www.stevenabbott.co.uk/practical-solubility/effects.php>.
- 48) Gao, P., & Mackley, M. R. (1991). Effect of pre solvent loading on the ultimate drawability of ultra-high molecular weight polyethylene. *Polymer*, 32 (17), 3136-3139.

Appendix A - Mechanical properties of DD1 fibers

In this section the procedure to determine mechanical properties was described, next the results of DD1 fibers were graphed.

The Favimat (filament tensile tester) determines the single filament linear density by the vibroscopic method and subsequently carries out the tensile test on exactly the same piece of single filament. In this way, specific tensile strengths can be tested very reliably and straightforwardly on single filaments. The clamping situation in the Favimat is given schematically in Figure 50.

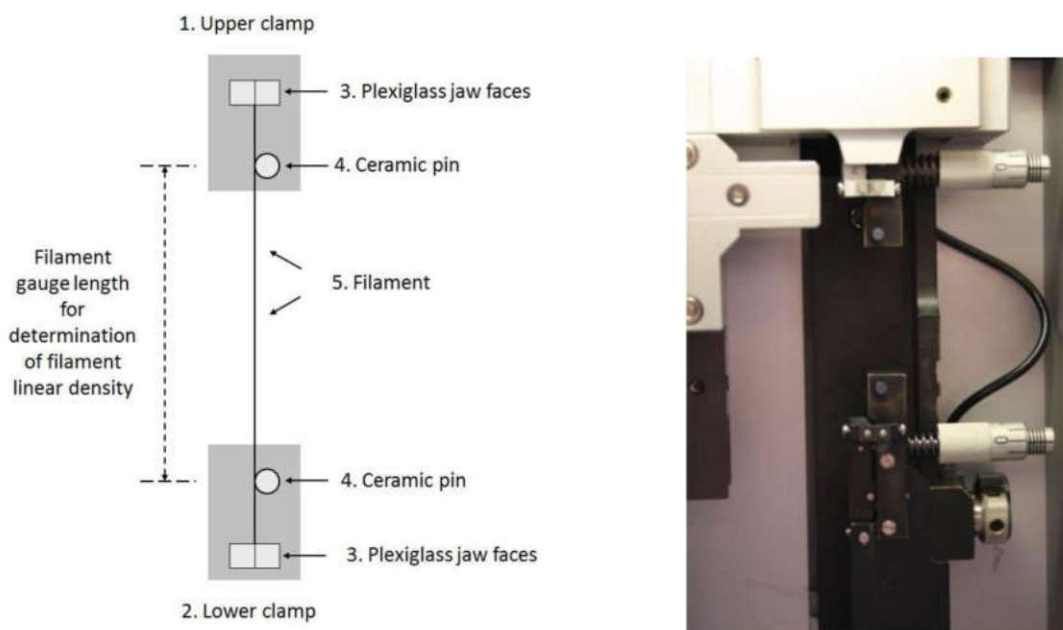


Figure 37: Schematic (a) clamping set-up of Favimat (b) test area in favimat

Both on the upper and lower clamp, the single UHMWPE filament is clamped between plexiglass jaw faces, and subsequently wrapped around a ceramic pin. The upper clamp is connected to a load cell. Prior to tensile testing, the vibroscope determines the filament linear density by measuring the resonating frequency of the transversal vibration induced by sound. Tensile testing is subsequently carried out by displacement of the lower clamp. For determination of modulus and strain, the whole sample length between the upper and lower plexiglass jaw faces was taken into account.

Thus the fully drawn fibers made in decalin, paraffin oil and solvent B were tested under favimat, and the obtained results were plotted below.

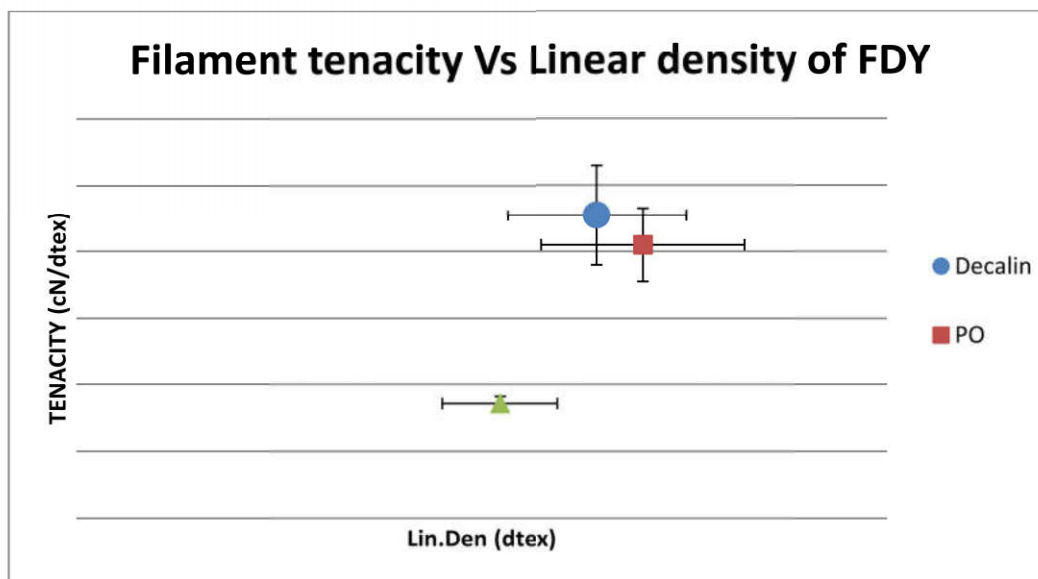


Figure 38: Filament tenacity versus linear density of fully drawn DD1 fibers made in decalin, PO and solvent B.

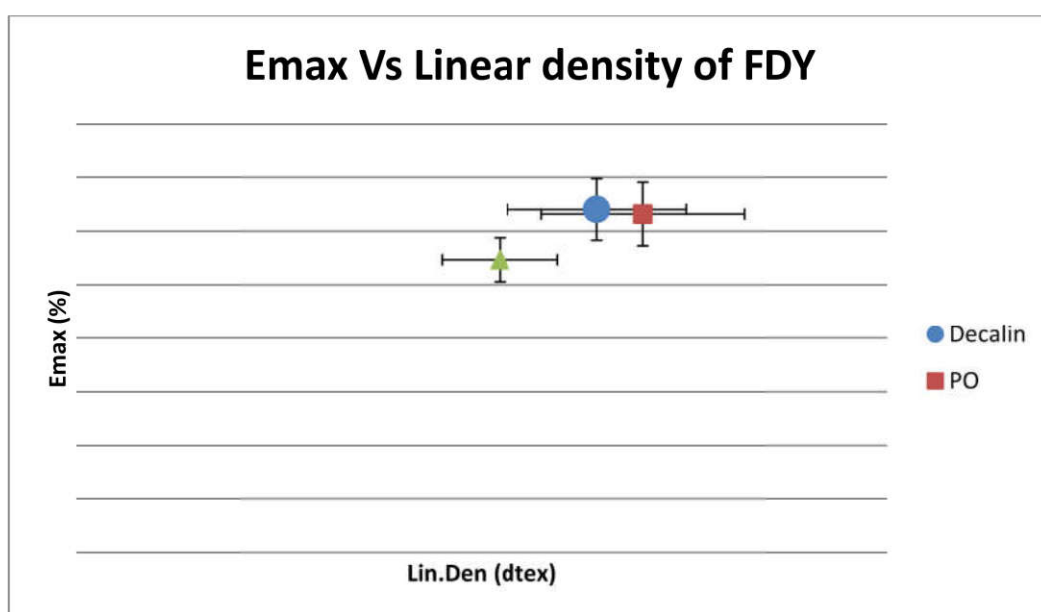


Figure 39: Elongation at break versus linear density of fully drawn DD1 fibers made in decalin, PO and solvent B.

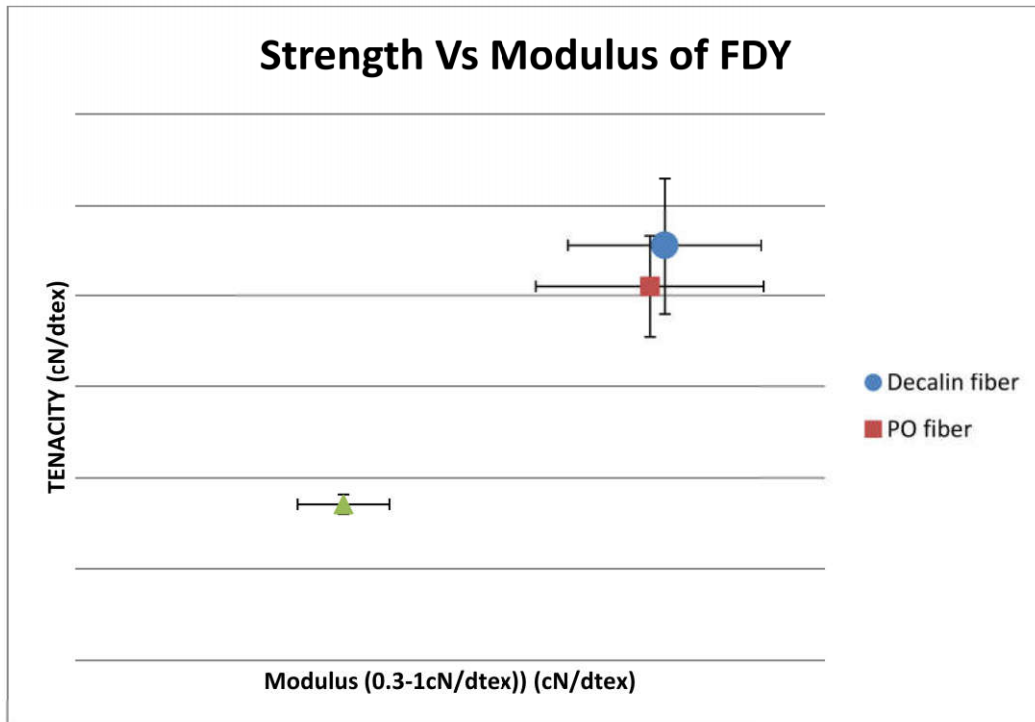


Figure 40: Tensile strength versus storage modulus of fully drawn DD1 fibers made in decalin, PO and solvent B.

The following conclusions can be drawn:

- Linear density's, tenacities and Moduli values of decalin and paraffin oil fibers were almost same (with in the experimental accuracy).
- Liner density of solvent B filaments is relatively low when compared to decalin and PO filaments (note that all of them have similar maximum draw ratios).
- Although tenacity of solvent B filaments scales with linear density, it is expected to have higher tenacities (almost equal to decalin filament's tenacity).
- Additional to degradation, other factors like morphology obtained during draw down could also play an important role in this strange behavior of solvent B filament properties.

Appendix B - SEM of DD1 fibers

Here, the SEM pictures of the cross section of undrawn solvent free fibers made in decalin, paraffin oil and stearic acid were shown.

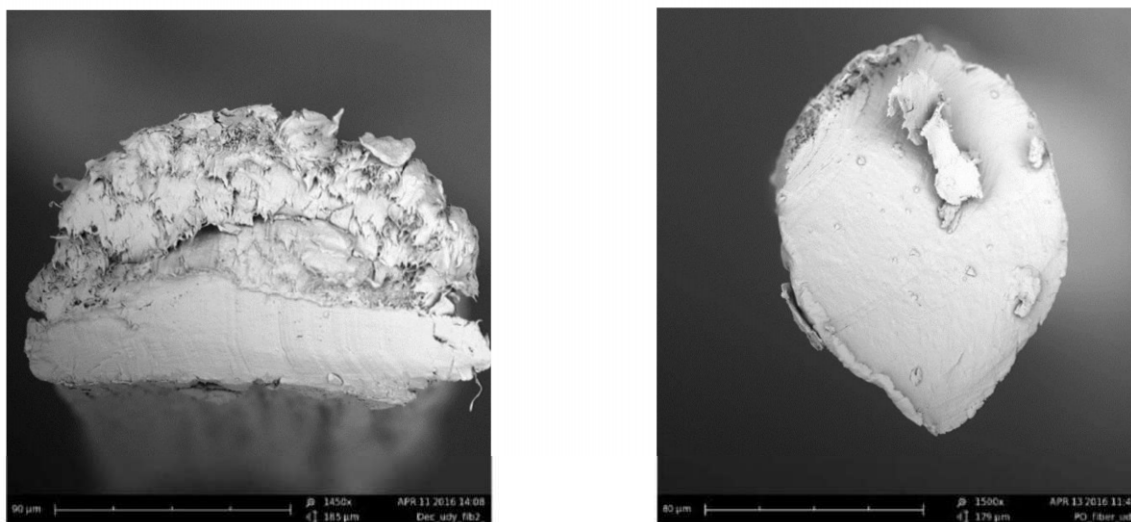


Figure 41: SEM pictures of DD1 fiber made from (a) decalin at 1450x (b) Paraffin oil at 1500x



Figure 42: SEM picture of DD1 fiber made from stearic acid at 1450x

Although these fibers were cut in the liquid nitrogen to have clear surface to study the cross section under SEM, since the fibers are very thin, the knife smeared the surface which made us difficult to analyze the topology of fibers. Efficient way has to be used to understand the topology, as it may indicate some defects in fibers which lead to its undrawability.

Appendix C - Solvent extraction process in DD1 fibers

During the extraction of paraffin oil and stearic acid, it was found that the length of the fiber wound wooden bobbin is larger than the grey bin (the bin used for solvent extraction), see Figure 56. So the fiber was wound to a smaller bobbin and the used for solvent extraction. Due to the availability, a plastic bobbin was used here (Figure 57). It could be possible that the transfer of fiber to different bobbins during extraction, damage (crack) could have initiated in the fiber which results in earlier breakage: undrawable.



Figure 43 : Grey bin (left side) and black wooden bobbin (right side).



Figure 44: plastic bobbin used for extraction of solvents from fibers

Appendix D - Dissolution (flask) experiment

In this section, the flask experimental setup is explained (shown in Figure 58). This experiments were performed to validate melting point of dissolution obtained from DSC results. First, solution of UHMWPE in a solvent was prepared in a glass flask with a magnetic stirrer in it. This flask is dipped inside the oil bath, then the temperature of the oil is gradually increased. There was also N₂ flush into the flask to avoid oxidation of the polymer. At certain temperature, the polymer starts to dissolve in the solvent and forms a gel together, this temperature is considered as the melting point of dissolution (T_{m1}).

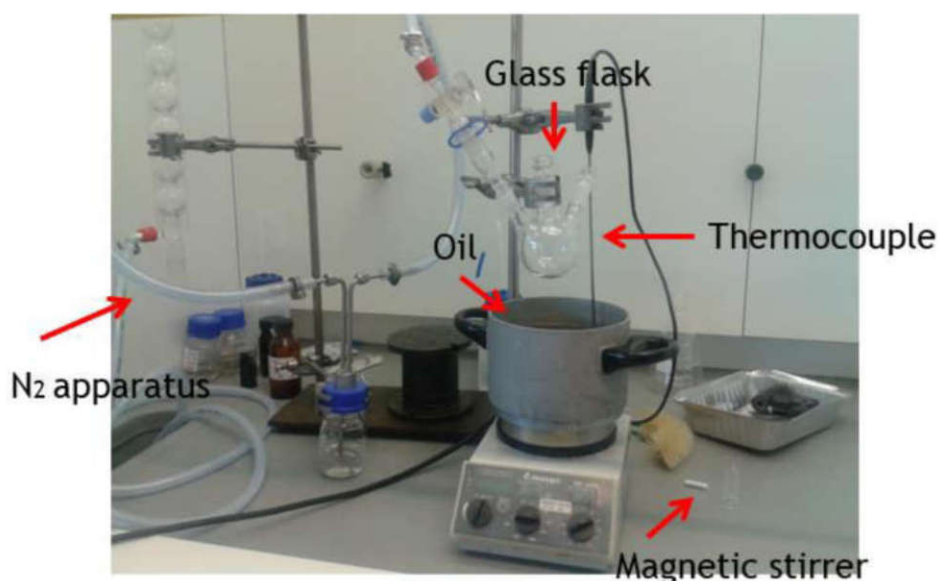


Figure 45: Experimental setup to obtain dissolution temperature (T_m).

For example, a solution of 10% UHMWPE in 90% paraffin oil was prepared and flask experiment was above experiment was performed. At 133°C, UHMWPE dissolved in paraffin oil and a gel is formed (see Figure 59). From DSC, melting point of dissolution was around 132 °C which is in line with flask experiment result.



Figure 46: the formation of gel with 10%UHMWPE in PO at 133°C